LA-UR-12-22977
Approved for public release; distribution is unlimited.

Title: The Mimetic Finite Element Method and the Virtual Element Method for elliptic problems with arbitrary regularity.

Author(s): Manzini, Gianmarco

Intended for: Report

# THE MIMETIC FINITE DIFFERENCE METHOD AND THE VIRTUAL ELEMENT METHOD FOR ELLIPTIC PROBLEMS WITH ARBITRARY REGULARITY

L. BEIRÃO DA VEIGA * AND G. MANZINI †

**Abstract.** We develop and analyze a new family of virtual element methods on unstructured polygonal meshes for the diffusion problem in primal form, that use arbitrarily regular discrete spaces $V_h \subset C^\alpha$, $\alpha \in \mathbb{N}$. The degrees of freedom are (a) solution and derivative values of various degree at suitable nodes and (b) solution moments inside polygons. The convergence of the method is proven theoretically and an optimal error estimate is derived. The connection with the Mimetic Finite Difference method is also discussed. Numerical experiments confirm the convergence rate that is expected from the theory.

**Key words.** Diffusion problem, virtual element method, polygonal mesh, Galerkin method, high-order scheme

**1. Introduction.** In this work, we investigate a very appealing feature of the *Virtual Element Method* (VEM) proposed in [6]: the design of numerical schemes that incorporate a given degree $\alpha \in \mathbb{N}$ of $C^\alpha$ global regularity into the discrete solution.66 Indeed, the discrete spaces of the conforming Finite Element Method are traditionally globally continuous, i.e., only $C^0$, and the construction of more regular elements, e.g., $C^1$ elements, is a very difficult task. Successful $C^1$ discretizations date back to mid sixties - early seventies and were obtained by using either a high polynomial degree, as, e.g., in the *Argyris and Bell* triangle [2, 15, 29], or a very complex design, as, e.g., the *HCT* triangle [30, 29]. Moreover, using such strategies to obtain a finite element space with $C^2$ or higher regularity becomes totally prohibitive. On the authors knowledge, the only technology that has succeeded later on in building piecewise polynomial and highly regular spaces is that of splines [32, 36] and the isogeometric analysis [31], but at the cost of using tensor product meshes or resorting to much more complex construction as that of *T-splines*.

The virtual element approach in [6] offers a strong alternative to such constructions: the finite element spaces that we will consider in this work are *virtual* is the sense that we do not need to build the basis functions explicitly to implement these methods. This feature allows us to design a family of numerical methods that are associated with discrete spaces with arbitrary $C^\alpha$ regularity and are suitable to very general unstructured polygonal meshes. To this end, we propose a new VEM that depends on two integer parameters, $\alpha$ for the regularity and $m$ for the polynomial degree of the approximation, with the minimal condition that $m \geq \alpha + 1$. The parameter $\alpha$ determines the global smoothness of the underlying discrete space, i.e., $C^\alpha$ regularity across the edges of the mesh. The parameter $m$ determines the order of convergence of the method in the energy norm, which is expected to be $\mathcal{O}(h^m)$ for sufficiently regular solution. Moreover, the convergence is also attained in higher order Sobolev norms; thus, the pointwise convergence of derived quantities, for example, e.g., gradients, may be guaranteed depending on the smoothness of the exact solution. Due to the VEM general approach, the convergence theory of our schemes is very similar

* Dipartimento di Matematica F. Enriques, Università degli Studi di Milano, via Saldini 50, 20133 Milano, Italy, e-mail: lourenco.beirao@unimi.it

† Istituto di Matematica Applicata e Tecnologie Informatiche (IMATI) – CNR, via Ferrata 1, I – 27100 Pavia, Italy e-mail: Marco.Manzini@imati.cnr.it

to that presented in [6], the main difference coming from the more general diffusion tensor $\mathsf{K}$ considered herein.

Although the present paper is complete, in the sense that it fully analyzes the method, we rather prefer to intend this contribution as a first exploration into a new direction. Indeed, the possibility to develop highly regular methods can pave the way to a wide range of applications. At a first glance, the main advantages offered by the VEM rely in simpler discretization of higher order problems, see, e.g., [19] and in the straightforward computation of derived quantities such as fluxes, strains, stresses, etc., which are directly related to the degrees of freedom of the numerical method. Other possible developments regard the anisotropic error estimation based on the Hessian of the solution and the construction of finite element spaces that exactly satisfy given constraints, as, for example, in the stream function formulation of the Stokes problem, where the velocity is the curl of a $C^1$ scalar field. We can also devise a VEM for better eigenvalue approximation, as studies in isogeometric analysis have shown that highly regular discrete spaces may give a better approximation of the high end of the spectrum. Finally, the present construction can be extended to a general "*hkp* approach", i.e. a method in which the polynomial degree may vary from element to element and the regularity index $\alpha$ may vary from edge to edge.

These goals may be achieved by keeping at the same time the property of mesh generality of the *Mimetic Finite Difference* (MFD) methods, see, e.g., the mixed and primal formulations given in [20, 17, 12]. The Virtual Element Method can, indeed, be considered as a Galerkin reformulation of arbitrary order Mimetic Finite Difference (MFD) method proposed in [12]. This fact is of primary importance since it establishes a clear and well-defined bridge between the nodal MFD methods and the finite element framework. However, such reformulations for mixed and nodal MFD methods would allow to extend the many fields where the mimetic technology has been successful to the VEM, as, for instance, the numerical solution of mixed and primal diffusion problems [20, 17, 10, 14, 13], of advection-diffusion problems [24, 8], of eigenvalue problems [22], of the obstacle problems [1], of the steady Stokes model [9, 11], of magnetostatic problems [34] and Maxwell equations [18], as well as the design of residual-based a posteriori estimators [4] using a post-processed solution [23] and of monotonicity criteria for the mixed-hybrid mimetic formulations [35]. Other higher-order mimetic schemes were also developed in [3, 27, 28, 25, 26] for the Support Operator Method (SOM) [37, 38], which is a precursor of the MFD method.

The outline of the paper is as follows. In Section 2 we introduce the mathematical model. In Section 3 we present the formulation of the new Virtual Element Method here proposed. In Section 4 we present the convergence analysis of the scheme. In Section 6 we confirm the theoretical results with numerical experiments. In Section 7 we offer final remarks and conclusions.

**2. The mathematical model.** Let us consider the steady diffusion problem for the scalar solution field $u$ given by

$$\operatorname{div}(\mathsf{K}\nabla u) = f \quad \text{in } \Omega, \tag{2.1}$$

$$u = g \quad \text{on } \Gamma, \tag{2.2}$$

where $\Omega \subset \mathbb{R}^2$ is the computational domain, $\Gamma$ is the boundary of $\Omega$, $\mathsf{K}$ is the diffusion tensor describing the material properties, $f$ is the forcing term and $g$ are the Dirichlet data. For simplicity of exposition, we will focus on the case of homogeneous Dirichlet boundary conditions, i.e., $g = 0$. The more general case is a straightforward extension and will be considered for the numerical experiments in Section 6.

We assume that:

(H1) $\Omega$ is a bounded, open, polygonal subset of $\mathbb{R}^2$;

(H2) the diffusion tensor $\mathsf{K} : \Omega \to \mathbb{R}^{2\times 2}$ is a $2 \times 2$ bounded, measurable, and symmetric tensor. Moreover, we assume that $\mathsf{K}$ is *strongly elliptic*, i.e., there exist two positive constants $\kappa_*$ and $\kappa^*$ such that for every $\mathbf{x} \in \Omega$ it holds

$$\kappa_* \|\mathbf{v}\|^2 \leq \mathbf{v} \cdot \mathsf{K}(\mathbf{x})\mathbf{v} \leq \kappa^* \|\mathbf{v}\|^2 \qquad \forall \mathbf{v} \in \mathbb{R}^2, \tag{2.3}$$

where $\|\mathbf{v}\|$ is the usual Euclidean norm of the vector $\mathbf{v}$.

(H3) the function $f$ belongs to $L^2(\Omega)$.

Throughout the paper, we will follow the usual notation for Sobolev spaces and norms (see e.g. [29]). In particular, for an open bounded domain $\mathcal{D}$, we will use $|\cdot|_{s,\mathcal{D}}$ and $|\cdot|_{s,\mathcal{D}}$ to denote seminorm and norm, respectively, in the Sobolev space $H^s(\mathcal{D})$, while $(\cdot,\cdot)_{0,\mathcal{D}}$ will denote the $L^2(\mathcal{D})$ inner product. Often the subscript will be omitted when $\mathcal{D}$ is the computational domain $\Omega$. Moreover, we represent the set of polynomials of degree *at most* $j$ on $\mathsf{P}$ by $\mathbb{P}_j(\mathsf{P})$ and the set of polynomials of degree *exactly equal to* $j$ by $\widehat{\mathbb{P}}_j(\mathsf{P})$. Finally, $\pi_j^{\mathcal{D}}$ will denote the usual $L^2(\mathcal{D})$- projection onto $\mathbb{P}_j(\mathcal{D})$, $j \in \mathbb{N}$.

Let us now consider the functional space $H_0^1(\Omega) = \{v \in H^1(\Omega),\ v_{|\Gamma} = 0\}$. Problem (2.1)-(2.2) can be restated in the variational form:

*find* $u \in H_0^1(\Omega)$ *such that*

$$\mathcal{A}\big(u, v\big) = \big(f, v\big) \qquad \forall v \in H_0^1(\Omega), \tag{2.4}$$

where

$$\mathcal{A}\big(u, v\big) = \int_\Omega \mathsf{K}\nabla u \cdot \nabla v \, dV \quad \text{and} \quad \big(f, v\big) = \int_\Omega f v \, dV.$$

Under assumptions (H1)-(H3), the bilinear form $\mathcal{A}$ is continuous and coercive and the linear functional $\big(f, \cdot\big)$ is continuous, thus implying the well-posedness of problem (2.4), i.e., existence and uniqueness of the weak solution [33].

**3. The discrete problem.** Let $\{\Omega_h\}_h$ be a sequence of decompositions of $\Omega$ into elements $\mathsf{P}$ labeled by the mesh size parameter $h$. For the moment, we assume that each decomposition $\Omega_h$ is made of a finite number of *simple polygons*, i.e., open simply connected sets whose boundary is a non intersecting line made of a finite number of straight line segments.

For every $h$, we construct a finite dimensional space $V_h \subset H_0^1(\Omega)$, and a bilinear form $\mathcal{A}_h :\ V_h \times V_h \to \mathbb{R}$ such that the discrete problem:

*Find* $u_h \in V_h$ *such that:*

$$\mathcal{A}_h\big(u_h, v_h\big) = \big(f_h, v_h\big)_h, \qquad \forall\, v_h \in V_h \tag{3.1}$$

has a unique solution $u_h$, and we have "good" approximation properties. If $m \geq 1$ is the target degree of accuracy, and the solution $u$ of (2.4) is smooth enough, we want to have

$$\|u - u_h\|_1 \leq C\, h^m |u|_{m+1}, \tag{3.2}$$

where $C$, here and in the following, is, as usual, a positive constant independent of $h$.

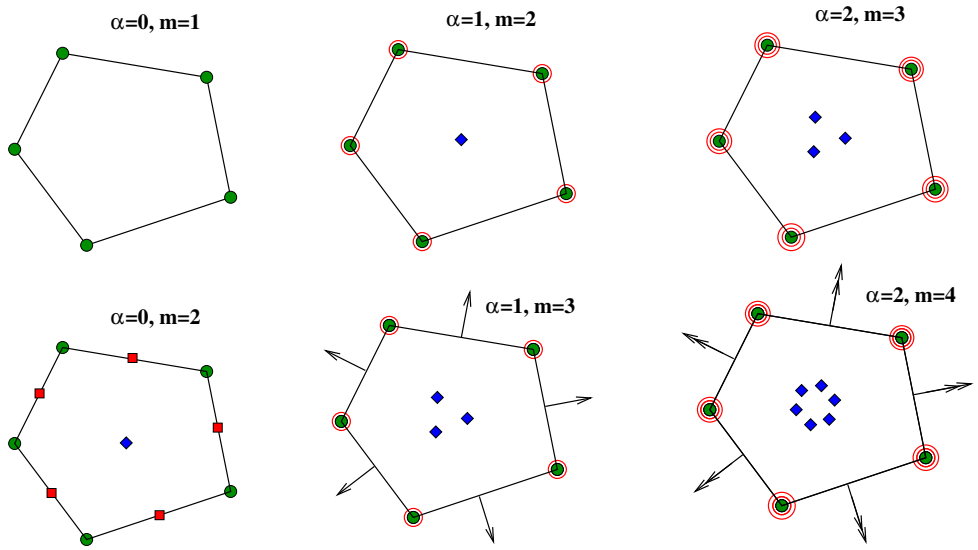


FIG. 3.1. *Degrees of freedom for $\alpha = 0, 1, 2$ and $m = \alpha + 1, \alpha + 2$. The symbols shown in the plots represent vertex values (dot), vertex first-order derivatives (one circle), vertex first- and second-order derivatives (two circles), edge values (square), first-order normal derivatives (arrow), first- and second-order normal derivatives (double arrow)*

**3.1. Local discrete spaces.** We denote a generic mesh vertex by $\mathsf{v}$ and its coordinate vector by $\mathbf{x}_\mathsf{v}$, a generic mesh edge by $\mathsf{e}$ and its length by $|\mathsf{e}|$, the area of polygon $\mathsf{P}$ by $|\mathsf{P}|$, and its boundary by $\partial\mathsf{P}$. The orientation of each edge $\mathsf{e}$ is reflected by its unit normal vector $\mathbf{n}_\mathsf{e}$, which is fixed once and for all. For any polygon $\mathsf{P}$ and any edge $\mathsf{e}$ of $\partial\mathsf{P}$, we define the unit normal vector $\mathbf{n}_{\mathsf{P},\mathsf{e}}$ that points out of $\mathsf{P}$. We denote the set of mesh vertices by $\mathcal{V}$ and the set of mesh edges by $\mathcal{E}$.

We refer to the integer number $\alpha \geq 0$ as the *regularity index* and to the integer number $m \geq \alpha + 1$ as the *consistency index*. For any integer $s \geq 0$, we define the functional space

$$\mathbb{B}_s(\partial\mathsf{P}) := \left\{ v \in L^2(\partial\mathsf{P}) \,:\, v_{|\mathsf{e}} \in \mathbb{P}_s(\mathsf{e}),\, \forall \mathsf{e} \in \partial\mathsf{P} \right\}.$$

Now, let $\alpha_j := \max\{2(\alpha - j) + 1, m - j\}$, so that, for example, $\alpha_0 := \max\{2\alpha + 1, m\}$ and $\alpha_1 := \max\{2\alpha - 1, m - 1\}$. We define the operator $\nabla^j v$ as the *collection of the derivatives of order $j$* of the scalar function $v$, with the usual convention that the zero-th order derivative coincides with the function. Thus, for example, it holds that $\nabla^0 v = v$, while $\nabla^1 v$ is the gradient of $v$, $\nabla^2 v$ is the hessian, etc. For each polygonal cell $\mathsf{P}$ and any pair of indices $(\alpha, m)$ with $\alpha \geq 0$ and $m \geq \alpha + 1$ we consider the local finite element space:

$$V_\mathsf{P}^{\alpha,m} = \Bigg\{ v \in H^{1+\alpha}(\mathsf{P}) \text{ with } \Delta^{1+\alpha} v \in \mathbb{P}_{m-2}(\mathsf{P}) \text{ s. t. for } j = 0, \ldots, \alpha$$

$$\text{there holds } \frac{\partial^j v}{\partial n^j}\Big|_{\partial\mathsf{P}} \in \mathbb{B}_{\alpha_j}(\partial\mathsf{P}), \nabla^j v_{|\partial\mathsf{P}} \in C^0(\partial\mathsf{P}) \Bigg\}, \tag{3.3}$$

with the convention that $\mathbb{P}_{-1}(\mathsf{P}) = \{0\}$ and where $\Delta^{1+\alpha}$ represents the Laplace operator $\Delta$ applied $(1 + \alpha)$ times.

Let us illustrate the meaning of this definition through a couple of examples. For $\alpha = 0$ and $m \geq 1$ we obtain the finite element spaces introduced in [6], which allow for the formulation of a family of schemes that are equivalent to arbitrary order mimetic method in [12]. In particular, for $m = 1$ we have the low-order nodal MFD method [**?**]. The functions that belong to these spaces are the solutions of the equation $\Delta v = p$ with $p \in \mathbb{P}_{m-2}(\mathsf{P})$ inside each polygonal cell $\mathsf{P}$, and their trace on the boundary $\partial\mathsf{P}$ is a continuous piecewise polynomial of degree $m$. For $\alpha = 1$ and $m = 2$, we obtain the finite element space of functions in $H^2(\mathsf{P})$ that satisfy the following conditions:

- the trace on the boundary of $\mathsf{P}$ is continuous and is a piecewise polynomial of degree $\alpha_0 = 3$;
- the normal derivative on each edge is a polynomial of degree $\alpha_1 = 1$;
- the gradient on the boundary is continuous;
- inside $\mathsf{P}$ these functions satisfy the bi-harmonic equation $\Delta^2 v = p$ with $p \in \mathbb{R}$.

REMARK 3.1. *The local space $V_{\mathsf{P}}^{\alpha,m}$ in* (3.3) *is virtual in the sense that we will not need to build it explicitly in order to implement the family of schemes here proposed.*

REMARK 3.2. *Note that $\Delta^{1+\alpha} v = div(\nabla(\Delta^\alpha v))$, and the integration by parts yields*

$$\int_{\mathsf{P}} \left(\Delta^{1+\alpha} u\right) v \, dV = -\int_{\mathsf{P}} \nabla(\Delta^\alpha u) \cdot \nabla v \, dV + \int_{\partial\mathsf{P}} \mathbf{n}_{\mathsf{P}} \cdot \nabla(\Delta^\alpha u)\, v \, dS.$$

**3.2. Local degrees of freedom.** We distinguish three kinds of degrees of freedom that are associated with each polygonal cell $\mathsf{P}$:

- $\mathcal{V}_{\mathsf{P}}^{\alpha,m}$: *vertex* degrees of freedom of $\mathsf{P}$;
- $\mathcal{E}_{\mathsf{P}}^{h}$: *edge* degrees of freedom of $\mathsf{P}$;
- $\mathcal{P}_{\mathsf{P}}^{h}$: *interior* degrees of freedom of $\mathsf{P}$.

In Figure 3.1 we depict some sample choices of degrees of freedom on a pentagonal element for $\alpha = 0, 1, 2$ and $m = \alpha + 1, \alpha + 2$.

*Vertex degrees of freedom.* The vertex degrees of freedom of a function $v$ associated with the vertex $\mathsf{v}$ are the partial derivatives $\nabla^j v(\mathsf{v})$ for $j = 0, 1, \ldots, \alpha$ of degree up to $\alpha$ evaluated at $\mathbf{x}_{\mathsf{v}}$. For instance, for $\alpha = 1$ we consider the value of $v(\mathbf{x}_{\mathsf{v}})$ and $\nabla v(\mathbf{x}_{\mathsf{v}})$ at each vertex $\mathsf{v}$ of $\partial\mathsf{P}$. For each mesh vertex, the total number of such degrees of freedom is given by $(\alpha + 1)(\alpha + 2)/2$.

*Edge degrees of freedom.* Let us consider a set of $\mathcal{N}_j^{\alpha,m}$ distinct nodes $\{\mathbf{x}_i\}_{i=1,\ldots,\mathcal{N}_j^{\alpha,m}}$ on the open edge $\mathsf{e}$, where

$$\mathcal{N}_j^{\alpha,m} = \max(m - (\alpha + 1) - (\alpha - j), 0) \tag{3.4}$$

for $\alpha \geq 0$, $m \geq \alpha + 1$, and $j = 0, \ldots, \alpha$, These points can be uniformly spaced along $\mathsf{e}$ or chosen as the nodes of suitable integration rules like those provided by Gauss-Lobatto formulas, cf. [12]. For each $j = 0, \ldots, \alpha$, the edge degrees of freedom of a function $v$ are given by the $\mathcal{N}_j^{\alpha,m}$ normal derivatives $\partial^j v(\mathbf{x}_k)/\partial n^j$ evaluated at these points (as usual, for $j = 0$ we take the function value). For each edge $\mathsf{e}$ of $\partial\mathsf{P}$, the total number of such degrees of freedom is given by

$$\frac{(m - \alpha + \beta)(m - \alpha - 1 - \beta)}{2} + \beta \qquad \text{where } \beta = \max\{m - (2\alpha + 1), 0\}.$$

When $m = \alpha + 1$ there are no edge degrees of freedom.

*Internal degrees of freedom.* Let $\mathbf{s} = (s_1, s_2)$ denote a two-dimensional multi-index with the usual notation $|\mathbf{s}| := s_1 + s_2$ and $\mathbf{x}^{\mathbf{s}} = x_1^{s_1} x_2^{s_2}$ when $\mathbf{x} = (x_1, x_2)$. For $m > 1$ we consider the set of $m(m-1)/2$ monomials

$$\mathcal{M}_{m-2} = \left\{ \left( \frac{\mathbf{x} - \mathbf{x}_{\mathsf{P}}}{h_{\mathsf{P}}} \right)^{\mathbf{s}}, \, |\mathbf{s}| \leq m-2 \right\}, \tag{3.5}$$

which is a basis for $\mathbb{P}_{m-2}(\mathsf{P})$. The *internal degrees of freedom* of the function $v$ are the moments:

$$\frac{1}{|\mathsf{P}|} \int_{\mathsf{P}} q(\mathbf{x})\, v(\mathbf{x}) \, dV \qquad \forall q \in \mathcal{M}_{m-2}(\mathsf{P}).$$

The total number of internal degrees of freedom is $m(m-1)/2$.

The dimension of the local space $V_{\mathsf{P}}^{\alpha,m}$ equals the total number of degrees of freedom of $\mathcal{V}_{\mathsf{P}}^{\alpha,m}$ plus $\mathcal{E}_{\mathsf{P}}^{h}$ plus $\mathcal{P}_{\mathsf{P}}^{h}$

$$\mathcal{N}_{\mathsf{P}}^{\alpha,m} = N_{\mathsf{P}}^{\mathcal{E}} \Big( \frac{(\alpha+1)(\alpha+2)}{2} + \frac{(m-\alpha)(m-\alpha-1)}{2} \Big) + \frac{m(m-1)}{2}, \tag{3.6}$$

where $N_{\mathsf{P}}^{\mathcal{E}}$ is the number of edges of the polygon $\mathsf{P}$.

REMARK 3.3. *The degrees of freedom $\mathcal{V}_{\mathsf{P}}^{\alpha,m}$ plus $\mathcal{E}_{\mathsf{P}}^{h}$ uniquely determine a polynomial of degree $\alpha_0$ on each edge $\mathsf{e}$ of $\mathsf{P}$ representing the function value, and also polynomials of degree $\alpha_j$, $j = 1, 2, .., \alpha$, representing the $j^{th}$ normal derivative along the edge. In other words, $\mathcal{V}_{\mathsf{P}}^{\alpha,m}$ plus $\mathcal{E}_{\mathsf{P}}^{h}$ are equivalent to prescribe $\partial^j v / \partial n^j$ on $\partial\mathsf{P}$, for $j = 0, 1, .., \alpha$. On the other hand, the degrees of freedom $\mathcal{P}_{\mathsf{P}}^{h}$ are equivalent to prescribe $\pi_{m-2}^{\mathsf{P}}(v)$ in $\mathsf{P}$. We recall that $\pi_{m-2}^{\mathsf{P}}$ is the projection operator, in the $L^2(\mathsf{P})$ norm, onto the space $\mathbb{P}_{m-2}(\mathsf{P})$.*

For the space $V_{\mathsf{P}}^{\alpha,m}$ and the degrees of freedom $\mathcal{V}_{\mathsf{P}}^{\alpha,m}$ plus $\mathcal{E}_{\mathsf{P}}^{h}$ plus $\mathcal{P}_{\mathsf{P}}^{h}$ we have the following *unisolvence result.*

PROPOSITION 3.1. *Let $\mathsf{P}$ be a simple polygon with $N_{\mathsf{P}}^{\mathcal{E}}$ edges, and let the space $V_{\mathsf{P}}^{\alpha,m}$ be defined as in* (3.3)*. The degrees of freedom $\mathcal{V}_{\mathsf{P}}^{\alpha,m}$ plus $\mathcal{E}_{\mathsf{P}}^{h}$ plus $\mathcal{P}_{\mathsf{P}}^{h}$ are unisolvent for $V_{\mathsf{P}}^{\alpha,m}$.*

*Proof.* The present proof is very similar to the analogous one in [6]. We present it for completeness. According to Remark 3.3, to prove the proposition it is enough to see that a function $v \in V_{\mathsf{P}}^{\alpha,m}$ such that

$$\frac{\partial^j v}{\partial n^j} = 0 \qquad \text{on } \partial\mathsf{P}, \quad \forall \mathsf{P} \in \Omega_h, \, j = 0, 1, .., \alpha, \tag{3.7}$$

and

$$\pi_{m-2}^{\mathsf{P}}(v) = 0 \qquad \text{in } \mathsf{P}, \quad \forall \mathsf{P} \in \Omega_h, \tag{3.8}$$

is actually identically zero in $\mathsf{P}$. In order to prove this, we show that $\Delta^{1+\alpha} v = 0$ in $\mathsf{P}$ (that joined with (3.7) gives $v \equiv 0$). To this end, we first solve, for every $q \in \mathbb{P}_{m-2}(\mathsf{P})$, the following auxiliary problem:

$$\begin{aligned} \sigma \, \Delta^{1+\alpha} w &= q \qquad \text{in } \mathsf{P}, \\ \frac{\partial^j w}{\partial n^j} &= 0 \qquad \text{on } \partial\mathsf{P}, \text{ for } j \in [0, \alpha] \end{aligned} \tag{3.9}$$

where $\sigma = (-1)^{1+\alpha}$. This problem is reformulated in variational form as follows:

$$\textit{find } w \in H_0^{1+\alpha}(\mathsf{P}) \textit{ such that}: \qquad \mathcal{B}_{\mathsf{P}}\big(w, v\big) = (q, v)_{0,\mathsf{P}} \qquad \forall v \in H_0^{1+\alpha}(\mathsf{P}), \quad (3.10)$$

with $\mathcal{B}_{\mathsf{P}}$ denoting the elliptic bilinear form associated to the operator $\sigma\Delta^{1+\alpha}$ on $\mathsf{P}$ through an integration by parts, cf. Remark 3.2. Note that (3.9) can be written as $w = \sigma\Delta_{0,\mathsf{P}}^{-1-\alpha}(q)$, the latter symbol representing the inverse operator.

Next, we consider the map $R$, from $\mathbb{P}_{m-2}(\mathsf{P})$ into itself, defined by

$$R(q) := \pi_{m-2}^{\mathsf{P}}\big(\sigma\Delta_{0,\mathsf{P}}^{-1-\alpha}(q)\big) \equiv \pi_{m-2}^{\mathsf{P}}(w). \quad (3.11)$$

We claim that $R$ is an isomorphism. Indeed, from (3.11), the definition of $\pi_{m-2}^{\mathsf{P}}$, and (3.10) we have, for every $q \in \mathbb{P}_{m-2}(\mathsf{P})$:

$$(R(q), q)_{0,\mathsf{P}} = \big(\pi_{m-2}^{\mathsf{P}}\big(\sigma\Delta_{0,\mathsf{P}}^{-1-\alpha}(q)\big), q\big)_{0,\mathsf{P}} = \big(\pi_{m-2}^{\mathsf{P}}(w), q\big)_{0,\mathsf{P}} = (w, q)_{0,\mathsf{P}} = \mathcal{B}_{\mathsf{P}}\big(w, w\big).$$

Since $w$ is in $H_0^{1+\alpha}(\mathsf{P})$ we have then that

$$R(q) = 0 \;\Leftrightarrow\; \mathcal{B}_{\mathsf{P}}\big(w, w\big) = 0 \;\Leftrightarrow\; w = 0 \;\Leftrightarrow\; q = 0. \quad (3.12)$$

We notice that, if $\partial^j v/\partial n^j = 0$ on $\partial\mathsf{P}$, $j = 0, \ldots, \alpha$, then

$$\pi_{m-2}^{\mathsf{P}}(v) = \pi_{m-2}(\sigma\Delta_{0,\mathsf{P}}^{-1-\alpha}(\sigma\Delta^{1+\alpha}v)) = R(\sigma\Delta^{1+\alpha}v).$$

Hence, $\pi_{m-2}^{\mathsf{P}}(v) = 0 \Longrightarrow R(\sigma\Delta^{1+\alpha}v) = 0 \Longrightarrow \sigma\Delta^{1+\alpha}v = 0$, and the proof is concluded. □

REMARK 3.4. *We obtain a better condition number of the stiffness matrix, and we also simplify its construction (see Section 3.4), by scaling the nodal degrees of freedom as follows. Let $\nu$ be a vertex or an edge node of $\mathsf{P} \in \Omega_h$. We set*

$$h_\nu = \max_{\mathsf{P}:\nu\in\partial\mathsf{P}} h_{\mathsf{P}}.$$

*Then, we rescale all the degrees of freedom that are derivatives of order $j$ in $\nu$ by $h_\nu^j$.*

**3.3. Construction of the finite element space $V_h$.** We can now design $V_h$, the *virtual element space* on the whole domain $\Omega$. For every decomposition $\Omega_h$ of $\Omega$ into simple polygons $\mathsf{P}$ and for every integer $k \geq 1$ we first define the *space without boundary conditions*.

$$W_h = \{v \in H^{1+\alpha}(\Omega) \;:\; v_{|\mathsf{P}} \in V_{\mathsf{P}}^{\alpha,m}\ \forall \mathsf{P} \in \Omega_h\}. \quad (3.13)$$

In agreement with the local choice of the degrees of freedom, in $W_h$ we choose the following *degrees of freedom*:

- $\mathcal{V}^h$: the value of $\nabla^j v_h$, $j = 0, \ldots, \alpha$, at the vertices of $\mathcal{V}/\Gamma$;
- $\mathcal{E}^h$: the value of $\partial^j v_h/\partial n^j$ for $j = 0, \ldots, \alpha$ at the $\mathcal{N}_j^{\alpha,m}$ internal nodes of each edge of $\mathcal{E}/\Gamma$, where $\mathcal{N}_j^{\alpha,m}$ is defined in (3.4);
- $\mathcal{P}^h$: the value of the moments

$$\frac{1}{|\mathsf{P}|}\int_{\mathsf{P}} q(\mathbf{x})v_h(\mathbf{x})\,dV \qquad \forall q \in \mathcal{M}_{m-2}(\mathsf{P}),\ m \geq 2$$

in each polygonal cell $\mathsf{P}$, where the set $\mathcal{M}_{m-2}(\mathsf{P})$ is defined in (3.5).

Finally, the discrete space $V_h$ is given by

$$V_h = \Big\{ v \in H_0^{1+\alpha}(\Omega) \ : \ v_{|\mathsf{P}} \in V_{\mathsf{P}}^{\alpha,m} \ \forall \mathsf{P} \in \Omega_h \Big\}. \tag{3.14}$$

Note that the condition $v_h \in V_h$ implies $v_h = 0$ on the vertices and the edges of the boundary $\Gamma$. Therefore, the degrees of freedom of $V_h$ are simply the ones introduced above, excluding the nodal degrees of freedom associated with function values (not the derivatives) of the boundary vertices and edges. The dimension of $V_h$ equals the total number of degrees of freedom for vertices, edges and elements. Proposition 3.1 implies that the global degrees of freedom are unisolvent for the global space $V_h$.

**3.4. Construction of $\mathcal{A}_h$.** We build the discrete bilinear form $\mathcal{A}_h$ through the assembly of the local bilinear forms $\mathcal{A}_{h,\mathsf{P}}$ in accordance with

$$\mathcal{A}_h\big(w_h, v_h\big) = \sum_{\mathsf{P} \in \Omega_h} \mathcal{A}_{h,\mathsf{P}}\big(w_h, v_h\big) \qquad \forall w_h, v_h \in V_h. \tag{3.15}$$

The local bilinear forms $\mathcal{A}_{h,\mathsf{P}}$ are all *symmetric* and satisfy the following fundamental properties of *consistency* and *stability*.

- **Consistency:** for all $h$, for all $\mathsf{P}$ in $\Omega_h$, and $m \geq 1$ it holds

$$\mathcal{A}_{h,\mathsf{P}}\big(p, v_h\big) = \int_\Omega \big(\pi_{m-1}^{\mathsf{P}}(\mathsf{K}\nabla p)\big) \cdot \nabla v_h \, dV \qquad \forall p \in \mathbb{P}_m(\mathsf{P}), \ \forall v_h \in V_{\mathsf{P}}^{\alpha,m}. \tag{3.16}$$

- **Stability**: there exist two positive constants $\alpha_*$ and $\alpha^*$, independent of $h$ and $\mathsf{P}$, such that

$$\alpha_* \, \mathcal{A}_{\mathsf{P}}\big(v_h, v_h\big) \leq \mathcal{A}_{h,\mathsf{P}}\big(v_h, v_h\big) \leq \alpha^* \, \mathcal{A}_{\mathsf{P}}\big(v_h, v_h\big) \qquad \forall v_h \in V_{\mathsf{P}}^{\alpha,m}. \tag{3.17}$$

Note that in the present paper we consider a more general diffusion tensor $\mathsf{K}$ with respect to [6], that is the reason for the modified consistency condition (3.16). Nevertheless, in the case that $\mathsf{K}_{|\mathsf{P}}$ is constant, the projection operator $\pi_{m-1}^{\mathsf{P}}$ in (3.16) can be neglected, thus giving

$$\mathcal{A}_{h,\mathsf{P}}\big(p, v_h\big) = \mathcal{A}_{\mathsf{P}}\big(p, v_h\big) \qquad \forall p \in \mathbb{P}_m(\mathsf{P}), \ \forall v_h \in V_{\mathsf{P}}^{\alpha,m}.$$

First of all, let us observe that the local degrees of freedom allow us to compute exactly $\mathcal{A}_{h,\mathsf{P}}\big(p, v_h\big)$ for any $p \in \mathbb{P}_m(\mathsf{P})$ and for any $v_h \in V_{\mathsf{P}}^{\alpha,m}$. Indeed, let us assume (3.16) and integrate by parts

$$\begin{aligned} \mathcal{A}_{h,\mathsf{P}}\big(p, v_h\big) &= \int_\Omega \big(\pi_{m-1}^{\mathsf{P}}(\mathsf{K}\nabla p)\big) \cdot \nabla v \, dV \\ &= -\int_{\mathsf{P}} \operatorname{div}\big(\pi_{m-1}^{\mathsf{P}}(\mathsf{K}\nabla p)\big) \, v_h \, dV + \int_{\partial\mathsf{P}} \mathbf{n}_{\mathsf{P}} \cdot \big(\pi_{m-1}^{\mathsf{P}}(\mathsf{K}\nabla p)\big) \, v_h \, dS. \end{aligned} \tag{3.18}$$

Since $\operatorname{div}\big(\pi_{m-1}^{\mathsf{P}}(\mathsf{K}\nabla p)\big) \in \mathbb{P}_{m-2}(\mathsf{P})$, the first integral in the right-hand side of (3.18) can be expressed through the polynomial moments of $v_h$, and can, thus, be computed exactly by using its internal degrees of freedom. On the other hand, it holds that $\mathbf{n}_{\mathsf{P}} \cdot \big(\pi_{m-1}^{\mathsf{P}}(\mathsf{K}\nabla p)\big) \in \mathbb{P}_{m-1}(\mathsf{e})$ and $v_{h|\mathsf{e}} \in \mathbb{P}_{\alpha_0}(\mathsf{e})$ for all $\mathsf{e} \subset \partial\mathsf{P}$, and the second integral in the right-hand side of (3.18) can be computed exactly. Therefore, the bilinear form $\mathcal{A}_h$ can be computed exactly without knowing $v_h$ in the interior of $\mathsf{P}$.

At this point, we are left to show how to construct a (computable!) $\mathcal{A}_h$ that satisfies (3.16) and (3.17). For any $\mathsf{P} \in \Omega_h$ and for any sufficiently regular function $\varphi$ we set

$$\overline{\varphi} := \frac{1}{N_{\mathsf{P}}^{\mathcal{V}}} \sum_{i=1}^{N_{\mathsf{P}}^{\mathcal{V}}} \varphi(\mathbf{x}_{\mathsf{v}_i}) \tag{3.19}$$

where $\mathbf{x}_{\mathsf{v}_i}$ is the position vector of $\mathsf{v}_i$, the $i$-th vertex of $\partial\mathsf{P}$ in a local numbering system for $i$ running from 1 to $N_{\mathsf{P}}^{\mathcal{V}}$.

Next, we define the operator $\Pi_m^{\mathsf{P}} : \ V_{\mathsf{P}}^{\alpha,m} \longrightarrow \mathbb{P}_m(\mathsf{P}) \subset V_{\mathsf{P}}^{\alpha,m}$ as the solution of

$$\mathcal{A}_{\mathsf{P}}\big(\Pi_m^{\mathsf{P}}(v_h), q\big) = \int_\Omega \big(\pi_{m-1}^{\mathsf{P}}(\mathsf{K}\nabla q)\big) \cdot \nabla v_h \, dV \quad \forall q \in \mathbb{P}_m(\mathsf{P}) \tag{3.20}$$

$$\overline{\Pi_m^{\mathsf{P}}(v_h)} = \overline{v_h}, \tag{3.21}$$

for all $v_h \in V_{\mathsf{P}}^{\alpha,m}$. Equations (3.20)-(3.21) imply that:

$$\Pi_m^{\mathsf{P}}(p) = p, \quad \forall p \in \mathbb{P}_m(\mathsf{P}), \tag{3.22}$$

since the first equation will tell us that $p$ and $\Pi_m^{\mathsf{P}}(p)$ have the same gradient, and the second equation takes care of the constant part.

At this point, choosing $\mathcal{A}_{h,\mathsf{P}}\big(u, v\big) = \mathcal{A}_{\mathsf{P}}\big(\Pi_m^{\mathsf{P}}(u), \Pi_m^{\mathsf{P}}(v)\big)$ for any couple of functions $u$ and $v$ would ensure property (3.16), but (3.17) in general would not be verified. We need to add a term able to ensure (3.17). Let then $S^{\mathsf{P}}(u, v)$ be any symmetric positive definite bilinear form to be chosen to verify

$$c_0 \mathcal{A}_{\mathsf{P}}\big(v, v\big) \leq S^{\mathsf{P}}(v, v) \leq c_1 \mathcal{A}_{\mathsf{P}}\big(v, v\big) \quad \forall v \in V_{\mathsf{P}}^{\alpha,m} \quad \text{with } \Pi_m^{\mathsf{P}}(v) = 0 \tag{3.23}$$

for some positive constants $c_0,\ c_1$ independent of $\mathsf{P}$ and $h_{\mathsf{P}}$. Then, set

$$\mathcal{A}_{h,\mathsf{P}}\big(u, v\big) = \mathcal{A}_{\mathsf{P}}\big(\Pi_m^{\mathsf{P}}(u), \Pi_m^{\mathsf{P}}(v)\big) + S^{\mathsf{P}}(u - \Pi_m^{\mathsf{P}}(u), v - \Pi_m^{\mathsf{P}}(v)) \quad \forall u, v \in V_{\mathsf{P}}^{\alpha,m}. \tag{3.24}$$

Then, the following lemma is immediate to check.

LEMMA 3.2. *The bilinear form* (3.24) *satisfies the consistency property* (3.16) *and the stability property* (3.17).

In general, the choice of the bilinear form $S^{\mathsf{P}}$ would depend on the problem and on the degrees of freedom. From (3.23) it is clear that $S^{\mathsf{P}}$ must scale like $\mathcal{A}_{\mathsf{P}}$ on the kernel of $\Pi_m^{\mathsf{P}}$. For each element $\mathsf{P} \in \Omega_h$, we denote by $\chi_i$, $i = 1, \ldots, \mathcal{N}_{\mathsf{P}}^{\alpha,m}$ the operator that to each smooth enough function $\varphi$ associates the $i$-th local degree of freedom $\chi_i(\varphi)$ (we recall that $\mathcal{N}_{\mathsf{P}}^{\alpha,m}$ is defined in (3.6)). Then, choosing the canonical basis $\varphi_1, \ldots, \varphi_{\mathcal{N}_{\mathsf{P}}^{\alpha,m}}$ as

$$\chi_i(\varphi_j) = \delta_{ij}, \quad i, j = 1, \ldots, \mathcal{N}_{\mathsf{P}}^{\alpha,m}, \tag{3.25}$$

the local stiffness matrix is given by

$$\mathcal{A}_{h,\mathsf{P}}\big(\varphi_i, \varphi_j\big) = \mathcal{A}_{\mathsf{P}}\big(\Pi_m^{\mathsf{P}}(\varphi_i), \Pi_m^{\mathsf{P}}(\varphi_j)\big) + S^{\mathsf{P}}(\varphi_i - \Pi_m^{\mathsf{P}}(\varphi_i), \varphi_j - \Pi_m^{\mathsf{P}}(\varphi_j)). \tag{3.26}$$

In our case it is easy to check that there must hold $\mathcal{A}_{\mathsf{P}}\big(\varphi_i, \varphi_i\big) \simeq |\varphi_i|_{1,\mathsf{P}}^2 \simeq 1$ for each "*reasonable polygon*", i.e. any polygon satisfying the mesh assumptions discussed in Section 4. This property is true for all $i = 1, 2, \ldots, \mathrm{N}^{\mathsf{P}}$ since we properly scaled the

local degrees of freedom, see (3.5) and Remark 3.4. Therefore, a simple choice for $S^{\mathsf{P}}$ that satisfies (3.23) is given by

$$S^{\mathsf{P}}\big(\varphi_i - \Pi^{\mathsf{P}}_m(\varphi_i), \varphi_j - \Pi^{\mathsf{P}}_m(\varphi_j)\big) = \sum_{r=1}^{\mathcal{N}^{\alpha,m}_{\mathsf{P}}} \chi_r\big(\varphi_i - \Pi^{\mathsf{P}}_m(\varphi_i)\big)\chi_r\big(\varphi_j - \Pi^{\mathsf{P}}_m(\varphi_j)\big).$$

REMARK 3.5. *For all $p, q \in \mathbb{P}_m(\mathsf{P})$, from the definition of $\pi^{\mathsf{P}}_{m-1}$ and since $\nabla q \in \mathbb{P}_{m-1}(\mathsf{P})$, it follows*

$$\mathcal{A}_{h,\mathsf{P}}\big(p, q\big) = \int_\Omega \big(\pi^{\mathsf{P}}_{m-1}(\mathsf{K}\nabla q)\big) \cdot \nabla q \, dV = \int_\Omega (\mathsf{K}\nabla p) \cdot \nabla q \, dV = \mathcal{A}_{\mathsf{P}}\big(p, q\big).$$

*Therefore the bilinear form turns out to be exact when both entries are polynomials, even if $\mathsf{K}$ is not constant on the element $\mathsf{P}$. Note that the above identity also implies that the consistency condition is compatible with the symmetry of $\mathcal{A}^{\mathsf{P}}_h$, since it gives $\mathcal{A}_{h,\mathsf{P}}\big(p, q\big) = \mathcal{A}_{h,\mathsf{P}}\big(q, p\big)$ for all $p, q \in \mathbb{P}_m(\mathsf{P})$.*

**3.5. Construction of the loading term.** We consider first the case $m \geq 2$, and define $f_h$ on each element $\mathsf{P}$ as the $L^2(\mathsf{P})$-projection of $f$ onto the space $\mathbb{P}_{m-2}$, that is,

$$f_h = \pi^{\mathsf{P}}_{m-2}(f) \qquad \text{on each } \mathsf{P} \in \Omega_h.$$

Consequently, the associated right-hand side

$$\big(f_h, v_h\big)_h = \sum_{\mathsf{P}\in\Omega_h} \int_{\mathsf{P}} f_h \, v_h \, dV \equiv \sum_{\mathsf{P}\in\Omega_h} \int_{\mathsf{P}} \pi^{\mathsf{P}}_{m-2}(f) \, v_h \, dV = \sum_{\mathsf{P}\in\Omega_h} \int_{\mathsf{P}} f \, \pi^{\mathsf{P}}_{m-2}(v_h) \, dV$$

can be exactly computed using the degrees of freedom for $V_h$ that represent the internal moments. For $m = 1$ we approximate $f$ by a piecewise constant, and define

$$\big(f_h, v_h\big) = \sum_{\mathsf{P}\in\Omega_h} \int_{\mathsf{P}} \pi^{\mathsf{P}}_0(f) \, \overline{v}_h \, dV = \sum_{\mathsf{P}\in\Omega_h} |\mathsf{P}| \, \pi^{\mathsf{P}}_0(f) \, \overline{v}_h, \tag{3.27}$$

with $\overline{v}_h$ defined as in (3.19).

**4. Convergence analysis.** In this section we derive the convergence analysis of the method. We will make use of the following regularity assumption on the mesh.

*Mesh assumption.* We assume that there exists a real number $\gamma > 0$ such that, for all $h$, each element $\mathsf{P}$ in $\Omega_h$ is star-shaped with respect to a ball of radius $\geq \gamma h_{\mathsf{P}}$, where $h_{\mathsf{P}}$ is the diameter of $\mathsf{P}$. Moreover we assume that there exists a real number $\gamma' > 0$ such that, for all $h$ and for each element $\mathsf{P}$ in $\Omega_h$, the distance between any two vertices of $\mathsf{P}$ is $\geq \gamma' h_{\mathsf{P}}$.

REMARK 4.1. *The above mesh conditions can be relaxed. We refer the interested reader to [6] for a thourough discussion concerning this issue.*

We now consider the following discrete approximations of the solution $u$. For each element $\mathsf{P} \in \Omega_h$, we denote by $\chi_i$, $i = 1, \ldots, \mathcal{N}^{\alpha,m}_{\mathsf{P}}$ the operator that associates the $i$-th local degree of freedom $\chi_i(\varphi)$ to each smooth enough function $\varphi$. It follows that for every smooth enough function $w$ there exists a unique element $w^{\mathtt{I}}$ of $V^{\alpha,m}_{\mathsf{P}}$ such that

$$\chi_i(w - w^{\mathtt{I}}) = 0, \quad i = 1, \ldots, \mathcal{N}^{\alpha,m}_{\mathsf{P}}. \tag{4.1}$$

In the following we will make use of the interpolated field $u^{\mathtt{I}} \in V_h$. Finally, let $u_\pi$ be the $L^2$ projection of $u$ on the space of (discontinuous) functions that are piecewise polynomials of degree $m$ on the mesh $\Omega_h$.

The following convergence theorem holds.

THEOREM 4.1. *Let the consistency and stability assumptions* (3.16)-(3.17) *on the method and the conditions above on the mesh hold. Then, the discrete problem:*

Find $u_h \in V_h$ such that

$$\mathcal{A}_h\big(u_h, v_h\big) \;=\; \big(f_h, v_h\big)_h \qquad \forall\, v_h \in V_h, \tag{4.2}$$

*has a unique solution $u_h$.*
*Let moreover the tensor field $\mathsf{K}|_{\mathsf{P}} \in W^{s,\infty}(\mathsf{P})$ for all $\mathsf{P} \in \Omega_h$. Then, if the solution $u \in H^{1+\alpha}(\Omega)$, it holds*

$$|u - u_h|_1 \;\leq Ch^s\, |u|_{s+1} \tag{4.3}$$

*for all $1 + \alpha \leq s \leq m$, where $C$ is a constant independent of $h$.*

*Proof.* Existence and uniqueness of the solution of (4.2) is a consequence of (3.17) and of the coercivity of $\mathcal{A}$. To ease the notation, will use the symbol $\lesssim$ to indicate bounds up to a constant that is independent of $h$. Setting $\delta_h := u_h - u^{\mathtt{I}}$, using (4.2), (3.15), and adding and subtracting $u_\pi$ it follows

$$\begin{aligned} k_\star\alpha_*\, |\delta_h|_1^2 \leq \alpha_*\, \mathcal{A}\big(\delta_h, \delta_h\big) \leq \mathcal{A}_h\big(\delta_h, \delta_h\big) &= \mathcal{A}_h\big(u_h, \delta_h\big) - \mathcal{A}_h\big(u^{\mathtt{I}}, \delta_h\big) \\ &= \big(f_h, \delta_h\big)_h - \sum_{\mathsf{P}\in\Omega_h} \mathcal{A}_{h,\mathsf{P}}\big(u^{\mathtt{I}}, \delta_h\big) \\ &= \big(f_h, \delta_h\big)_h - \sum_{\mathsf{P}\in\Omega_h} \Big( \mathcal{A}_{h,\mathsf{P}}\big(u^{\mathtt{I}} - u_\pi, \delta_h\big) + \mathcal{A}_{h,\mathsf{P}}\big(u_\pi, \delta_h\big) \Big). \end{aligned} \tag{4.4}$$

From the above equation, first using (3.16) and then by some simple manipulation, we get

$$\begin{aligned} |\delta_h|_1^2 \lesssim |f_h|\, \delta_h - \sum_{\mathsf{P}\in\Omega_h} \Big( \mathcal{A}_{h,\mathsf{P}}\big(u^{\mathtt{I}} - u_\pi, \delta_h\big) + \mathcal{A}_{\mathsf{P}}\big(u_\pi, \delta_h\big) + T_1^{\mathsf{P}} \Big) \\ = \big(f_h, \delta_h\big)_h - \sum_{\mathsf{P}\in\Omega_h} \Big( \mathcal{A}_{h,\mathsf{P}}\big(u^{\mathtt{I}} - u_\pi, \delta_h\big) + \mathcal{A}_{\mathsf{P}}\big(u_\pi - u, \delta_h\big) + T_1^{\mathsf{P}} \Big) - \mathcal{A}\big(u, \delta_h\big), \end{aligned} \tag{4.5}$$

where we introduced the term

$$T_1^{\mathsf{P}} = \int_{\mathsf{P}} (\pi_{m-1}^{\mathsf{P}} - I)(\mathsf{K}\nabla u_\pi) \cdot \nabla \delta_h. \tag{4.6}$$

Now, recalling (2.4), the above bound yields

$$\begin{aligned} |\delta_h|_1^2 \lesssim \big(f_h, \delta_h\big)_h - \sum_{\mathsf{P}\in\Omega_h} \Big( \mathcal{A}_{h,\mathsf{P}}\big(u^{\mathtt{I}} - u_\pi, \delta_h\big) + \mathcal{A}_{\mathsf{P}}\big(u_\pi - u, \delta_h\big) + T_1^{\mathsf{P}} \Big) - \big(f, \delta_h\big) \\ = T_f - \sum_{\mathsf{P}\in\Omega_h} \Big( T_1^{\mathsf{P}} + T_2^{\mathsf{P}} + T_3^{\mathsf{P}} \Big). \end{aligned} \tag{4.7}$$

where the terms

$$T_f = \big(f_h, \delta_h\big)_h - \big(f, \delta_h\big) \tag{4.8}$$

$$T_2^{\mathsf{P}} = \mathcal{A}_{h,\mathsf{P}}\big(u^{\mathtt{I}} - u_\pi, \delta_h\big) \tag{4.9}$$

$$T_3^{\mathsf{P}} = \mathcal{A}_{\mathsf{P}}\big(u_\pi - u, \delta_h\big). \tag{4.10}$$

We need to bound the four terms above. By assuming that $f$ is sufficiently regular and using the same argument in [6, 7] we obtain the following approximation estimate:

$$\left|\left(f_h, v_h\right)_h - \left(f, v_h\right)\right| \lesssim h^s \Big( \sum_{\mathsf{P}\in\Omega_h} |f|^2_{s-1,\mathsf{P}} \Big)^{1/2}. \tag{4.11}$$

We thus obtain the inequality

$$|T_f| \lesssim \Big( h^s \sum_{\mathsf{P}\in\Omega_h} |f|_{s-1,\mathsf{P}} \Big) |\delta_h|_1 \lesssim h^s \, |u|_{s+1} \, |\delta_h|_1 \,. \tag{4.12}$$

By a triangle inequality and using the continuity of each $\mathcal{A}^{\mathsf{P}}$ and (3.17) we get

$$\left|T_2^{\mathsf{P}}\right| + \left|T_3^{\mathsf{P}}\right| \lesssim \Big( |u - u_\pi|_{1,\mathsf{P}} + \left|u - u^{\mathtt{I}}\right|_{1,\mathsf{P}} \Big) \, |\delta_h|_{1,\mathsf{P}} \,. \tag{4.13}$$

Given our mesh assumption, it is easy to check (following for instance the Scott-Dupont theory, see e.g. [16]) that the following approximation result holds

$$|u - u_\pi|_{1,\mathsf{P}} + \left|u - u^{\mathtt{I}}\right|_{1,\mathsf{P}} \lesssim h_{\mathsf{P}}^s \, |u|_{s+1,\mathsf{P}} \,. \tag{4.14}$$

Combining (4.13) with (4.14) gives the estimate

$$\left|T_2^{\mathsf{P}}\right| + \left|T_3^{\mathsf{P}}\right| \lesssim h_{\mathsf{P}}^s \, |u|_{s+1,\mathsf{P}} \, |\delta_h|_{1,\mathsf{P}} \,. \tag{4.15}$$

We finally bound the terms $T_1^{\mathsf{P}}$. We first note that by the Cauchy-Schwarz inequality

$$\left|T_1^{\mathsf{P}}\right| \leq \|(\pi^{\mathsf{P}}_{m-1} - I)(\mathsf{K}\nabla u_\pi)\|_{0,\mathsf{P}} \, |\delta_h|_{1,\mathsf{P}} \,. \tag{4.16}$$

By the triangle inequality and recalling the definition of $\pi^{\mathsf{P}}_{m-1}$ we get

$$\begin{aligned} \|(\pi^{\mathsf{P}}_{m-1} - I)(\mathsf{K}\nabla u_\pi)\|_{0,\mathsf{P}} &\leq \|(\pi^{\mathsf{P}}_{m-1} - I)(\mathsf{K}\nabla u)\|_{0,\mathsf{P}} + \|(\pi^{\mathsf{P}}_{m-1} - I)(\mathsf{K}\nabla u - \mathsf{K}\nabla u_\pi)\|_{0,\mathsf{P}} \\ &\leq \|(\pi^{\mathsf{P}}_{m-1} - I)(\mathsf{K}\nabla u)\|_{0,\mathsf{P}} + \|\mathsf{K}\nabla(u - u_\pi)\|_{0,\mathsf{P}}. \end{aligned} \tag{4.17}$$

Again by standard approximation estimates on polygons, applied to the two terms above, and recalling the regularity hypotheses on $\mathsf{K}$, from (4.17) it is easy to derive

$$\|(\pi^{\mathsf{P}}_{m-1} - I)(\mathsf{K}\nabla u_\pi)\|_{0,\mathsf{P}} \lesssim \left( h^s \, |u|_{s+1,\mathsf{P}} + |u - u_\pi|_{1,\mathsf{P}} \right) \lesssim h^s \, |u|_{s+1,\mathsf{P}} \,. \tag{4.18}$$

The bounds (4.16) and (4.18) yield

$$\left|T_1^{\mathsf{P}}\right| \lesssim h^s \, |u|_{s+1,\mathsf{P}} \, |\delta_h|_{1,\mathsf{P}} \,. \tag{4.19}$$

A bound for $|\delta_h|_1$ follows easily by combining (4.7) with (4.12), (4.15) and (4.19). Finally the result is obtained by a triangle inequality and again standard approximation results for $u - u^{\mathtt{I}}$. □

The following Corollary of Theorem 4.1 shows the convergence of $u_h$ to $u$ in terms of scaled higher order norms.

COROLLARY 4.2. *Under the same hypotheses of Theorem 4.1, for all* $0 \leq r \leq \alpha$ *it holds*

$$\sum_{\mathsf{P}\in\Omega_h} h_{\mathsf{P}}^r \, |u - u_h|_{r+1,\mathsf{P}} \leq C h^s \, |u|_{s+1} \tag{4.20}$$

*for all* $1+\alpha \leq s \leq m$*, where* $C$ *is a constant independent of* $h$*.*

*Proof.* We will only sketch the main ideas of the proof. Under the mesh assumptions above, it is easy to check that there is a uniform bound on the number of edges for all elements in the mesh family. Therefore, one can build a bounded number of reference polygons and, due to the shape regularity condition, uniformly regular mappings from each element of $\Omega_h$ to one of such reference polygons. This observation, together with the fact that the spaces $V_{\mathsf{P}}^{\alpha,m}$ are finite dimensional, allows us to make use of inverse estimates. Therefore, using also approximation estimates as in the previous proof, we get for all $\mathsf{P} \in \Omega_h$

$$\begin{aligned} h_{\mathsf{P}}^r \left|u-u_h\right|_{r+1,\mathsf{P}} &\leq h_{\mathsf{P}}^r \left|u^{\mathtt{I}}-u_h\right|_{r+1,\mathsf{P}} + h_{\mathsf{P}}^r \left|u-u^{\mathtt{I}}\right|_{r+1,\mathsf{P}} \\ &\lesssim \left|u^{\mathtt{I}}-u_h\right|_{1,\mathsf{P}} + h_{\mathsf{P}}^s \left|u\right|_{s+1,\mathsf{P}}. \end{aligned} \tag{4.21}$$

Taking the square, summing over all the elements and using the bound for $\left|u^{\mathtt{I}}-u_h\right|_1$ derived in the proof of Theorem 4.1, yields from (4.21)

$$\sum_{\mathsf{P}\in\Omega_h} \left|u-u_h\right|_{r+1,\mathsf{P}}^2 \lesssim h^s \left|u\right|_{s+1}.$$

The result now follows by a triangle inequality. ∎

REMARK 4.2. *We note that the interpolated field* $u^I$*, which we introduced at the beginning of this section, can also be defined in a different way, e.g., by using local integrals in accordance with the classical Clément approximation. In such a case, the element-wise locality of the approximation estimates is lost, but the regularity requirement for the solution* $u$ *is relaxed to* $u \in H^\alpha(\Omega)$*.*

Note that the regularity requirement on $u$ appearing in (4.3) is not realistic when $\mathsf{K}$ is discontinuous across the edges of the mesh $\Omega_h$. Indeed, it is well known from the approximation theory that in such a case a discrete space $V_h$ with $C^1$ or higher regularity is not the best choice. Nevertheless, the schemes considered herein can be easily adapted in order to make use of a less regular space $V_h$ across *selected vertices and edges* of the mesh. To this purpose, we consider the same degrees of freedom for each element $\mathsf{P}$, but those associated with first- or higher-order derivatives at the nodes of the chosen edges or at the selected vertices are no longer single-valued and may take different values when referred to different elements. This strategy requires to modify only the assembly of the global stiffness matrix while the construction of the local element matrices remains unchanged. The resulting discrete space $V_h$ will show a $C^0$-regularity only across the selected edges.

**5. Connection with the MFD method.** In this section, we show that the virtual element method considered in this work can be re-interpreted as a mimetic discretization that extends the high-order MFD method proposed in [12] to the case of arbitrary regular solutions. To this end, we present an alternative derivation of the bilinear form $\mathcal{A}_{h,\mathsf{P}}$ that considers only the degrees of freedom as is usual in the mimetic setting. Obviously, the degrees of freedom are the same of Section 3 and we use the same notation for the vertex and the edge ones. Instead, we relabel the local degrees of freedom that are related to the polynomial moments as follows. Let $v$ be a smooth function and $\mathsf{P}$ a given cell of $\Omega_h$. The function $\varphi_{k,i}$ is the monomial of $\mathcal{M}_{\alpha-2}(\mathsf{P})$ that corresponds to the multi-index $\mathbf{s} = (s_1, s_2)$ after setting that $k = |\mathbf{s}| = s_1 + s_2$ and $i = s_1$. The internal degree of freedom associated with this monomial is denoted

by $v_{\mathsf{P},k,i}$, and, formally, it holds that

$$v_{\mathsf{P},k,i} = \frac{1}{|\mathsf{P}|}\int_{\mathsf{P}} v\varphi_{k,i}\,dV, \qquad k=0,\dots,m-2, \quad i=0,1,\dots,k. \tag{5.1}$$

To ease notation, throughout the section, we will denote the *grid function* collecting the vertex, edge and internal degrees of freedom of a function $v_h$ of $V_h$ by the same symbol $v_h$, the grid functions collecting the degrees of freedom of a regular function $v$ by $v^{\mathtt{I}}$, the local bilinear forms acting on such grid functions by $\mathcal{A}_{h,\mathsf{P}}$ and the global bilinear form that is given by the assembly of the local ones by $\mathcal{A}_h$. We emphasize the fact that in this section $v_h$ and $v^{\mathtt{I}}$ are vectors (with real valued components representing the value of the degrees of freedom) instead of functions and that $\mathcal{A}_{h,\mathsf{P}}$ and $\mathcal{A}_h$ are matrices that multiply these vectors (they are, indeed, a matrix representation of the homonymous bilinear forms of subsection 3.4). The collection of all the grid functions defined on $\mathsf{P}$ with the obvious definition of sum of two grid functions and multiplication of a grid function by a scalar number is a linear space and will be denoted by $\mathcal{V}_{\mathsf{P}}^{\alpha,m}$.

**5.1. The mimetic bilinear form $\mathcal{A}_{h,\mathsf{P}}$.** In some respects, the mimetic derivation is very similar to the derivation of subsection 3.4. Our goal here is to emphasize the role of the degrees of freedom by noting that this alternative derivation does not make use of concepts like basis functions. Let us first assume, for simplicity of exposition, that $\mathsf{K}$ is a piecewise constant tensor with respect to the mesh partition of $\Omega$, i.e., that the restriction of $\mathsf{K}$ to each cell $\mathsf{P}$ is a constant tensor; the general case of a non-constant tensor will be discussed at the end of the subsection. In accordance with (3.15), the bilinear form $\mathcal{A}_h$ is provided by assembling the local *symmetric* bilinear forms $\mathcal{A}_{h,\mathsf{P}} : \mathcal{V}_{\mathsf{P}}^{\alpha,m} \times \mathcal{V}_{\mathsf{P}}^{\alpha,m} \to \mathbb{R}$ that are defined for each polygonal cell $\mathsf{P}$. Each bilinear form $\mathcal{A}_{h,\mathsf{P}}$ is an approximation of the local bilinear form

$$\mathcal{A}_{\mathsf{P}}\big(p,v\big) = \int_{\mathsf{P}} \nabla p\cdot\mathsf{K}\nabla v\,dV \quad p,v\in H^1(\mathsf{P}), \tag{5.2}$$

in the sense that

$$\mathcal{A}_{h,\mathsf{P}}\big(p^{\mathtt{I}},v^{\mathtt{I}}\big) \;=\; \mathcal{A}_{\mathsf{P}}\big(p,v\big) \tag{5.3}$$

when $p$ is a polynomial of degree $m$ and the function $v$ belongs to $V_{\mathsf{P}}^{\alpha,m}$. The exactness relation expressed by (5.3), which is the mimetic counterpart of the consistency condition expressed by (3.16) in the VEM context, is the crucial requirement whose satisfaction makes it possible to build the bilinear form $\mathcal{A}_{h,\mathsf{P}}$ directly on the degrees of freedom. To this purpose, we first reformulate (5.3) through an integration by parts that yields

$$\mathcal{A}_{\mathsf{P}}\big(p,v\big) = -\int_{\mathsf{P}} \mathrm{div}(\mathsf{K}\nabla p)\,v\,dV + \sum_{\mathsf{e}\in\partial\mathsf{P}}\int_{\mathsf{e}} (\mathbf{n}_{\mathsf{P},\mathsf{e}}\cdot\mathsf{K}\nabla p)v\,dS. \tag{5.4}$$

As $p$ is a polynomial of degree $m$ and $\mathsf{K}$ is a constant tensor field on $\mathsf{P}$, the divergence term, i.e., $\mathrm{div}(\mathsf{K}\nabla p)$ is also a polynomial of degree $(m-2)$. We express the divergence term $\mathrm{div}(\mathsf{K}\nabla p)$ as a linear combination of the monomials $\varphi_{k,i}$ in $\mathcal{M}_{m-2}(\mathsf{P})$ that form a basis of $\mathbb{P}_{m-2}(\mathsf{P})$ as

$$\mathrm{div}(\mathsf{K}\nabla p) = \sum_{k=0}^{m-2}\sum_{i=0}^{k} \alpha_{k,i}\,\varphi_{k,i}, \tag{5.5}$$

where the coefficients $\alpha_{k,i}$ of the decomposition may depend on $\mathsf{P}$. We substitute (5.5) into the first term in the right hand side of (5.4), and use the definition of the internal degrees of freedom for $v^{\mathtt{I}}$ given in (5.1). The left hand side of (5.6) can be expressed in terms of the internal degrees of freedom of $v^{\mathtt{I}}$ according to the development

$$
\begin{aligned}
-\int_{\mathsf{P}} \operatorname{div}(\mathsf{K}\nabla p)\, v\, dV &= -\sum_{k=0}^{m-2}\sum_{i=0}^{k} \alpha_{k,i} \int_{\mathsf{P}} \varphi_{k,i}\, v\, dV \\
&= -\sum_{k=0}^{m-2}\sum_{i=0}^{k} |\mathsf{P}|\, \alpha_{k,i}\, v_{\mathsf{P},k,i} =: \mathcal{I}_{\mathsf{P}}\big(v^{\mathtt{I}},\, p\big),
\end{aligned}
\tag{5.6}
$$

which also defines the cell quadrature rule $\mathcal{I}_{\mathsf{P}}\big(v^{\mathtt{I}},\, p\big)$.

Moreover, the trace of $v$ on each edge $\mathsf{e} \in \partial\mathsf{P}$ is a univariate polynomial of degree $m$, cf. definition (3.3), and is uniquely determined by the nodal and edges degrees of $\mathsf{e}$ by solving a polynomial interpolation problem. For every $v_h \in \mathcal{V}_{\mathsf{P}}^{\alpha,m}$, we denote the interpolation polynomial defined on the edge $\mathsf{e}$ of $\partial\mathsf{P}$ by $v_{\mathsf{e}}^{\mathtt{I}}(s)$, $s \in [0, |\mathsf{e}|]$, and we note the, formally, it holds that $v_{|\mathsf{e}} = v_{\mathsf{e}}^{\mathtt{I}}$. Hence, the second term in the right hand side of (5.4) can be written as

$$
\sum_{\mathsf{e}\in\partial\mathsf{P}} \int_{\mathsf{e}} (\mathbf{n}_{\mathsf{P},\mathsf{e}} \cdot \mathsf{K}\nabla p) v\, dS = \sum_{\mathsf{e}\in\partial\mathsf{P}} \int_{\mathsf{e}} (\mathbf{n}_{\mathsf{P},\mathsf{e}} \cdot \mathsf{K}\nabla p)(v^{\mathtt{I}})_{\mathsf{e}}\, dS =: \mathcal{I}_{\mathsf{e}}\big(v^{\mathtt{I}},\, p\big),
\tag{5.7}
$$

which also defines the edge quadrature rule $\mathcal{I}_{\mathsf{e}}\big(v^{\mathtt{I}},\, p\big)$. It is worth noting that $\mathcal{I}_{\mathsf{P}}\big(v^{\mathtt{I}},\, p\big)$ only involves the internal degrees of freedom of $v$ related to $\mathsf{P}$ and that $\mathcal{I}_{\mathsf{e}}\big(v^{\mathtt{I}},\, p\big)$ only involves the nodal (vertex plus edge) degrees of freedom of edge $\mathsf{e}$.

By combining (5.4) with (5.6) and (5.7), we prove the remarkable property that condition (5.3) is equivalent to

$$
\mathcal{A}_{h,\mathsf{P}}\big(p^{\mathtt{I}}, v^{\mathtt{I}}\big) \;=\; \mathcal{I}_{\mathsf{P}}\big(v^{\mathtt{I}},\, p\big) + \sum_{\mathsf{e}\in\partial\mathsf{P}} \mathcal{I}_{\mathsf{e}}\big(v^{\mathtt{I}},\, p\big). \qquad \text{for all } p, v \text{ as above.}
\tag{5.8}
$$

In other words, the value $\mathcal{A}_{\mathsf{P}}\big(p, v\big)$ only depends on the polynomial $p$ and the degrees of freedom $v^{\mathtt{I}}$, and is *independent of the specific functional form that $v$ takes inside* $\mathsf{P}$.

The consistency condition (S1) that we state below for each local bilinear form $\mathcal{A}_{h,\mathsf{P}}$ is a direct consequence of (5.8) as it extends such property to every mimetic field $v_h$. This condition is the mimetic counterpart of the virtual element condition (3.16) formulated for the case in which $\mathsf{K}$ is a constant tensor on $\mathsf{P}$, see also the development (3.18). In addition, we need the stability condition (S2) to guarantee the correct scaling and kernel for these discrete forms. This second condition correspond of the mimetic setting corresponds to the stability condition (3.17) of the virtual element setting. Each local bilinear form must be *symmetric* and is required to satisfy the following two conditions:

(S1) *local consistency*: for every $v_{h,\mathsf{P}} \in \mathcal{V}_{\mathsf{P}}^{\alpha,m}$ and for every $p \in \mathbb{P}_m(\mathsf{P})$ there holds:

$$
\mathcal{A}_{h,\mathsf{P}}\big(v_{h,\mathsf{P}}, p_{\mathsf{P}}^{\mathtt{I}}\big) = \mathcal{I}_{\mathsf{P}}\big(v_{h,\mathsf{P}},\, p\big) + \sum_{\mathsf{e}\in\partial\mathsf{P}} \mathcal{I}_{\mathsf{e}}\big(v_{h,\mathsf{P}},\, p\big).
\tag{5.9}
$$

(S2) *spectral stability*: there exists two positive constants $\sigma_*$ and $\sigma^*$ such that for every $v_{h,\mathsf{P}} \in \mathcal{V}_{\mathsf{P}}^{\alpha,m}$ there holds:

$$
\sigma_* \|v_{h,\mathsf{P}}\|_{1,h,\mathsf{P}}^2 \le \mathcal{A}_{h,\mathsf{P}}\big(v_{h,\mathsf{P}}, v_{h,\mathsf{P}}\big) \le \sigma^* \|v_{h,\mathsf{P}}\|_{1,h,\mathsf{P}}^2;
$$

$\alpha = 0$

| $m$ | dofs | conditions | interp. space |
|---|---|---|---|
| 1 |  | $2v_{\mathsf{v}}$ | $\mathbb{P}_1(\mathsf{e})$ |
| 2 |  | $2v_{\mathsf{v}} + v_{\mathsf{e}}$ | $\mathbb{P}_2(\mathsf{e})$ |
| 3 | 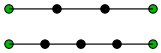 | $2v_{\mathsf{v}} + 2v_{\mathsf{e}}$ | $\mathbb{P}_3(\mathsf{e})$ |
| 4 |  | $2v_{\mathsf{v}} + 3v_{\mathsf{e}}$ | $\mathbb{P}_4(\mathsf{e})$ |

TABLE 5.1

*Degrees of freedom (dofs) for $\alpha = 0$ and $m = 1, 2, 3, 4$. Column dofs shows the number and kind of dofs for the pair $(\alpha, m)$ available for face $\mathsf{e}$; the symbols are the same used in Figure 3.1. Column conditions shows the type and number of conditions available to build such polynomial interpolation; the symbol $v_{\mathsf{v}}$ denotes the solution value at a vertex, the symbol $v_{\mathsf{e}}$ denotes the solution value at an internal node on the edge $\mathsf{e}$. Column interp. space show the interpolation space that can be built using the information available in the previous column.*

Conditions (S1) and (S2) are the mimetic counterpart to the assumptions of *consistency* and *stability* of subsection 3.4. Moreover, both conditions play a crucial role in the practical implementation of the method as we will see in the next subsections.

The previous derivation can be easily adapted to the case of a non-constant tensor field $\mathsf{K}$ on $\mathsf{P}$ by using the $L^2(\mathsf{P})$-orthogonal projector $\pi^{\mathsf{P}}_m$. For $p \in H^1(\mathsf{P})$ and $\mathsf{K} \in L^\infty(\mathsf{P})$ it holds that $\mathrm{div}(\pi^{\mathsf{P}}_{m-1}(\mathsf{K}\nabla p))$ belongs to $\mathbb{P}_{m-2}(\mathsf{P})$. Therefore, we can express this divergence as the unique linear combination of the polynomial basis functions $\varphi_{k,i}$ that form a basis of the polynomial space $\mathbb{P}_{m-2}(\mathsf{P})$:

$$\mathrm{div}(\pi^{\mathsf{P}}_{m-1}(\mathsf{K}\nabla p)) = \sum_{k=0}^{m-2} \sum_{i=0}^{k} \alpha_{k,i}\, \varphi_{k,i}, \tag{5.10}$$

where again the coefficients $\alpha_{k,i}$ of such decomposition may depend on $\mathsf{P}$. Then, we redefine the quadrature rule $\mathcal{I}_{\mathsf{P}}$ by using the coefficients $\alpha_{k,i}$ provided by (5.10) instead of those provided by formula (5.5). It is, thus, natural to modify the previous condition (S1) as follows:

(S1') *modified local consistency*: for every $v_{h,\mathsf{P}} \in \mathcal{V}^{\alpha,m}_{\mathsf{P}}$ and for every $p \in \mathbb{P}_m(\mathsf{P})$ there holds:

$$\mathcal{A}_{h,\mathsf{P}}\big(v_{h,\mathsf{P}}, p^{\mathrm{I}}_{\mathsf{P}}\big) = -\mathcal{I}_{\mathsf{P}}\big(v_{h,\mathsf{P}}, p\big) + \sum_{\mathsf{e}\in\partial\mathsf{P}} \int_{\mathsf{e}} v_{\mathsf{e}}(s)\, \pi^{\mathsf{P}}_{m-1}(\mathsf{K}\nabla p)\cdot \mathbf{n}_{\mathsf{P},\mathsf{e}}\, dS, \tag{5.11}$$

where $v_{\mathsf{e}}(s)$ is the (unique) polynomial of degree $m$ associated with the degrees of freedom in $v_{h,\mathsf{P}}$ associated with edge $\mathsf{e}$.

REMARK 5.1. *We point it out that condition (S1') is the mimetic formulation of the consistency condition* (3.16) *of the virtual element setting.*

REMARK 5.2. *Optionally, we could modify the definition of the edge quadrature rule $\mathcal{I}_{\mathsf{e}}\big(v^I, p\big)$ by introducing $\pi^{\mathsf{P}}_{m-1}$ in* (5.7) *and maintain the formulation of (S1).*

**5.2. Polynomial reconstructions along the edges.** Let $s \in [0, |\mathsf{e}|]$ be a local coordinate defined on the edge $\mathsf{e} = \overline{\mathsf{v}'\mathsf{v}''}$ and such that $s = 0$ corresponds to $\mathsf{v}'$ and $s = |\mathsf{e}|$ to $\mathsf{v}''$. The mimetic formulation of the method requires the reconstruction of the polynomial $v_{\mathsf{e}}(s)$ and its normal derivatives of order up to $\alpha$, here denoted for convenience as $\partial_n v_{\mathsf{e}}(s)$ when $j = 1$ and as $\partial^j_n v_{\mathsf{e}}(s)$ when $j = 2, \ldots, \alpha$. Such polynomials are obtained through suitable interpolation problems, which are designed for each edge to return the polynomials of *maximum degree* that can be determined

$\alpha = 1$

| $m$ | dofs | conditions | interp. space |
|---|---|---|---|
| 2 |  | $2v_{\mathsf{v}} + 2v'_{\mathsf{v}}$<br>$2\partial_n v_{\mathsf{v}}$ | $\mathbb{P}_3(\mathsf{e})$<br>$\mathbb{P}_1(\mathsf{e})$ |
| 3 |  | $2v_{\mathsf{v}} + 2v'_{\mathsf{v}}$<br>$2\partial_n v_{\mathsf{v}} + \partial_n v_{\mathsf{e}}$ | $\mathbb{P}_3(\mathsf{e})$<br>$\mathbb{P}_2(\mathsf{e})$ |
| 4 | 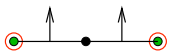 | $2v_{\mathsf{v}} + 2v'_{\mathsf{v}} + v_{\mathsf{e}}$<br>$2\partial_n v_{\mathsf{v}} + 2\partial_n v_{\mathsf{e}}$ | $\mathbb{P}_4(\mathsf{e})$<br>$\mathbb{P}_3(\mathsf{e})$ |
| 5 | 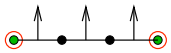 | $2v_{\mathsf{v}} + 2v'_{\mathsf{v}} + 2\partial_n v_{\mathsf{e}}$<br>$2\partial_n v_{\mathsf{v}} + 3\partial_n v_{\mathsf{e}}$ | $\mathbb{P}_5(\mathsf{e})$<br>$\mathbb{P}_4(\mathsf{e})$ |

TABLE 5.2

*Degrees of freedom for $\alpha = 1$ and $m = 2, 3, 4, 5$. Column* dofs *shows the number and kind of dofs for the pair $(\alpha, m)$ available for face $\mathsf{e}$; the symbols are the same used in Figure 3.1. Column* degree *shows the degree of $v_{|\mathsf{e}}$, the trace of a polynomial $v \in \mathbb{P}_m(\mathsf{P})$. Column* conditions *shows the type and number of conditions available to build such polynomial interpolation; the symbol $v_{\mathsf{v}}$ denotes the solution values at a vertex, $v_{\mathsf{e}}$ denotes the solution value at an internal node on the edge $\mathsf{e}$; $v'_{\mathsf{v}}$ denotes the tangential derivative at a vertex; $\partial_n v_{\mathsf{v}}$ and $\partial_n v_{\mathsf{e}}$ denotes the normal derivative at a vertex and at an internal node on the edge $\mathsf{e}$, respectively. Column* interp. space *show the interpolation space that can be built using the information available in the previous column.*

using the "*nodal + edge*" degrees of freedom available for that edge. A degree of freedom associated with a given vertex $\mathsf{v}$ is labeled by the subscript $\mathsf{v}$, e.g., $v_{\mathsf{v}}$ and $\nabla^j v_{\mathsf{v}}$ for $j > 0$. We will distinguish two cases: the *minimal* case, which corresponds to $m = \alpha + 1$, and the more general case, which corresponds to $m > \alpha + 1$.

*The minimal case $m = \alpha + 1$.* Let us be given the couple of indices $(\alpha, m)$ with $m = \alpha + 1$. This is the simplest situation because of the absence of the edge degrees of freedom and corresponds to the first row of Tables 5.1, 5.2, and 5.3. In such a case,

- $v_{\mathsf{e}}(s)$ depends on all the degrees of freedom associated with the vertices $\mathsf{v}'$ and $\mathsf{v}''$ of $\mathsf{e}$, i.e., the values of $v$ and on all the partial derivatives of order up to $\alpha$ (when $\alpha > 0$);
- $\partial_n^j v_{\mathsf{e}}(s)$ for $j \geq 1$ depends on the values of the partial derivatives of $v$ of order from $j$ to $\alpha$ in $\mathsf{v}'$ and $\mathsf{v}''$.

*Interpolation of the polynomial $v_{\mathsf{e}}(s)$.* To determine $v_{\mathsf{e}}$, we impose that the interpolated polynomial reproduces the value of $v$ and of the tangential derivatives of $v_{\mathsf{e}}$ of order up to $\alpha$ (when $\alpha > 0$) at $\mathsf{v}'$ and $\mathsf{v}''$. Hence, we have $(\alpha + 1)$ conditions to be imposed for each vertex, i.e., $2(\alpha + 1)$ conditions available for both vertices, and the degree of the polynomial is $(2\alpha + 1)$. For example,

- for $\alpha = 0$ (and $m = 1$), we consider only the two function values $v(\mathsf{v})$ for $\mathsf{v} \in \{\mathsf{v}', \mathsf{v}''\}$ and we impose the *two* conditions:

$$v_{\mathsf{e}}(0) = v(\mathsf{v}') \quad \text{and} \quad v_{\mathsf{e}}(|\mathsf{e}|) = v(\mathsf{v}''),$$

  which lead to a *linear* polynomial;
- for $\alpha = 1$ (and $m = 2$), we consider the function values and the first derivatives at each vertex, i.e., the *six* degrees of freedom $\big(v(\mathsf{v}), \nabla v(\mathsf{v})\big)$ for $\mathsf{v} \in \{\mathsf{v}', \mathsf{v}''\}$. We

$\alpha = 2$

| $m$ | dofs | conditions | interp. space |
|---|---|---|---|
| 3 |  | $2v_{\mathsf{v}} + 2v'_{\mathsf{v}} + 2v''_{\mathsf{v}}$ | $\mathbb{P}_5(\mathsf{e})$ |
| | | $2\partial_n v_{\mathsf{v}} + 2(\partial_n v_{\mathsf{v}})'$ | $\mathbb{P}_3(\mathsf{e})$ |
| | | $2\partial_n v_{\mathsf{v}}$ | $\mathbb{P}_1(\mathsf{e})$ |
| 4 |  | $2v_{\mathsf{v}} + 2v'_{\mathsf{v}} + 2v''_{\mathsf{v}}$ | $\mathbb{P}_5(\mathsf{e})$ |
| | | $2\partial_n v_{\mathsf{v}} + 2(\partial_n v_{\mathsf{v}})'$ | $\mathbb{P}_3(\mathsf{e})$ |
| | | $2\partial_n^2 v_{\mathsf{v}} + \partial_n^2 v_{\mathsf{e}}$ | $\mathbb{P}_2(\mathsf{e})$ |
| 5 |  | $2v_{\mathsf{v}} + 2v'_{\mathsf{v}} + 2v''_{\mathsf{v}}$ | $\mathbb{P}_5(\mathsf{e})$ |
| | | $2\partial_n v_{\mathsf{v}} + 2(\partial_n v_{\mathsf{v}})' + \partial_n v_{\mathsf{e}}$ | $\mathbb{P}_4(\mathsf{e})$ |
| | | $2\partial_n^2 v_{\mathsf{v}} + 2\partial_n^2 v_{\mathsf{e}}$ | $\mathbb{P}_3(\mathsf{e})$ |
| 6 | 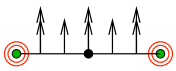 | $2v_{\mathsf{v}} + 2v'_{\mathsf{v}} + 2v''_{\mathsf{v}} + v_{\mathsf{e}}$ | $\mathbb{P}_6(\mathsf{e})$ |
| | | $2\partial_n v_{\mathsf{v}} + 2(\partial_n v_{\mathsf{v}})' + 2\partial_n v_{\mathsf{e}}$ | $\mathbb{P}_5(\mathsf{e})$ |
| | | $2\partial_n^2 v_{\mathsf{v}} + 3\partial_n^2 v_{\mathsf{e}}$ | $\mathbb{P}_4(\mathsf{e})$ |

TABLE 5.3

*Degrees of freedom for $\alpha = 2$ and $m = 3, 4, 5, 6$. Column* dofs *shows the number and kind of dofs for the pair $(\alpha, m)$ available for face $\mathsf{e}$; the symbols are the same used in Figure 3.1. Column* degree *shows the degree of $v_{|\mathsf{e}}$, the trace of a polynomial $v \in \mathbb{P}_m(\mathsf{P})$. Column* conditions *shows the type and number of conditions available to build such polynomial interpolation; the symbol $v_{\mathsf{v}}$ denotes the solution value at a vertex, $v_{\mathsf{e}}$ denotes the solution value at an internal node on the edge $\mathsf{e}$; $v'_{\mathsf{v}}$ and $v''_{\mathsf{v}}$ denote the first and second tangential derivative at a vertex; $\partial_n v_{\mathsf{v}}$ and $\partial_n v_{\mathsf{e}}$ denote the normal derivative at a vertex and at an internal node on the edge $\mathsf{e}$, while $(\partial_n v_{\mathsf{v}})'$ is the tangential derivative of $\partial_n v_{\mathsf{v}}(s)$ along $\mathsf{e}$; $\partial_n^2 v_{\mathsf{v}}$ and $\partial_n^2 v_{\mathsf{e}}$ denote the second normal derivative at a vertex and at an internal node on the edge $\mathsf{e}$. Column* interp. space *show the interpolation space that can be built using the information available in the previous column.*

impose the *four* conditions:

$$v_{\mathsf{e}}(0) = v(\mathsf{v}'), \qquad v_{\mathsf{e}}(|\mathsf{e}|) = v(\mathsf{v}''),$$
$$v'_{\mathsf{e}}(0) = \mathbf{t}_{\mathsf{e}} \cdot \nabla v(\mathsf{v}'), \qquad v'_{\mathsf{e}}(|\mathsf{e}|) = \mathbf{t}_{\mathsf{e}} \cdot \nabla v(\mathsf{v}''),$$

and we build a *cubic* polynomial;

- for $\alpha = 2$ (and $m = 3$), we consider the function values and the first and second derivatives at each vertex, i.e., the *twelve* degrees of freedom $\big(v(\mathsf{v}), \nabla v(\mathsf{v}), \nabla^2 v(\mathsf{v})\big)$ for $\mathsf{v} \in \{\mathsf{v}', \mathsf{v}''\}$. We impose the *six* conditions:

$$v_{\mathsf{e}}(0) = v(\mathsf{v}'), \qquad v_{\mathsf{e}}(|\mathsf{e}|) = v(\mathsf{v}''),$$
$$v'_{\mathsf{e}}(0) = \mathbf{t}_{\mathsf{e}} \cdot \nabla v(\mathsf{v}'), \qquad v'_{\mathsf{e}}(|\mathsf{e}|) = \mathbf{t}_{\mathsf{e}} \cdot \nabla v(\mathsf{v}''),$$
$$v''_{\mathsf{e}}(0) = \mathbf{t}_{\mathsf{e}} \cdot \nabla^2 v(\mathsf{v}')\mathbf{t}_{\mathsf{e}}, \qquad v''_{\mathsf{e}}(|\mathsf{e}|) = \mathbf{t}_{\mathsf{e}} \cdot \nabla^2 v(\mathsf{v}'')\mathbf{t}_{\mathsf{e}},$$

where we recall that $\nabla^2 v(\mathsf{v})$ stands for the hessian matrix of the function $v$ at the vertex $\mathsf{v}$, while $\mathbf{t}_{\mathsf{e}}$ is the tangent vector to $\mathsf{e}$ oriented from $\mathsf{v}'$ to $\mathsf{v}''$. In this case, we build an interpolation polynomial of degree 5.

*Interpolation of the polynomials $\partial_n^j v_{\mathsf{e}}(s)$ for $j = 1, \dots, \alpha$.* An analogous construction is made for the normal derivatives of order up to $\alpha$, i.e., for the polynomials $\partial_n^j v_{\mathsf{e}}$

on $\mathsf{e}$ with $1 \leq j \leq \alpha$. These polynomials are determined uniquely by imposing that they reproduce all the partial derivatives at $\mathsf{v}'$ and $\mathsf{v}''$ that can be constructed using all the available data at these vertices. For $j = \alpha$, i.e., the normal derivative with maximum order, we have only two conditions and *the interpolation is always linear*. For example,

- for $j = \alpha = 1$ (and $m = 2$), we construct $\partial_n v_{\mathsf{e}}(s)$ by imposing that

$$\partial_n v_{\mathsf{e}}(0) = \mathbf{n}_{\mathsf{e}} \cdot \nabla v(\mathsf{v}') \quad \text{and} \quad \partial_n v_{\mathsf{e}}(|\mathsf{e}|) = \mathbf{n}_{\mathsf{e}} \cdot \nabla v(\mathsf{v}'');$$

- for $j = \alpha = 2$ (and $m = 3$), we construct $\partial_n^2 v_{\mathsf{e}}(s)$ by imposing that

$$\partial_n^2 v_{\mathsf{e}}(0) = \mathbf{n}_{\mathsf{e}} \cdot \nabla^2 v(\mathsf{v}')\mathbf{n}_{\mathsf{e}} \quad \text{and} \quad \partial_n^2 v_{\mathsf{e}}(|\mathsf{e}|) = \mathbf{n}_{\mathsf{e}} \cdot \nabla^2 v(\mathsf{v}'')\mathbf{n}_{\mathsf{e}}.$$

Instead, for $1 < j < \alpha$ (when $\alpha > 1$), we can impose additional conditions by using the tangential derivatives of $\partial_n^j v_{\mathsf{e}}(s)$ along $\mathsf{e}$ at the vertices $\mathsf{v}'$ and $\mathsf{v}''$ to determine a unique interpolation polynomial. The degree of the resulting polynomial is always greater than one. We illustrate the case by the following examples:

- for $j = 0$, $\alpha = 1$ (and $m = 2$), we can set the *four* conditions

$$\begin{aligned} v_{\mathsf{e}}(0) &= v(\mathsf{v}'), & v_{\mathsf{e}}(|\mathsf{e}|) &= v(\mathsf{v}''), \\ v_{\mathsf{e}}'(0) &= \mathbf{t}_{\mathsf{e}} \cdot \nabla v(\mathsf{v}'), & v_{\mathsf{e}}'(|\mathsf{e}|) &= \mathbf{t}_{\mathsf{e}} \cdot \nabla v(\mathsf{v}''), \end{aligned}$$

- for $j = 1$, $\alpha = 2$ (and $m = 3$), we can set the *four* conditions

$$\begin{aligned} \partial_n v_{\mathsf{e}}(0) &= \mathbf{n}_{\mathsf{e}} \cdot \nabla v(\mathsf{v}'), & \partial_n v_{\mathsf{e}}(|\mathsf{e}|) &= \mathbf{n}_{\mathsf{e}} \cdot \nabla v(\mathsf{v}''), \\ \big(\partial_n v_{\mathsf{e}}\big)'(0) &= \mathbf{n}_{\mathsf{e}} \cdot \nabla^2 v(\mathsf{v}')\mathbf{t}_{\mathsf{e}}, & \big(\partial_n v_{\mathsf{e}}\big)'(|\mathsf{e}|) &= \mathbf{n} \cdot \nabla^2 v(\mathsf{v}'')\mathbf{t}_{\mathsf{e}}, \end{aligned}$$

that uniquely determine the interpolation polynomial $\partial_n v_{\mathsf{e}}(s)$ with degree 3. In general, in the minimal case the interpolation polynomials $\partial_n^j v_{\mathsf{e}}(s)$, $j = 0, 1, .., \alpha$ are of degree $2(\alpha - j) + 1$.

*The general case for $m > \alpha+1$.* . The situation is more complex when $m > \alpha+1$ as the edge degrees of freedom come into play in addition to the vertex conditions at $\mathsf{v}'$ and $\mathsf{v}''$ to build the polynomial trace reconstructions. More precisely,

- *for* $\alpha = 0$, we construct $v_{\mathsf{e}}(s)$ using $m - 1$ additional degrees of freedom that represent function evaluations at distinct points in the interior of $\mathsf{e}$, as shown in Table 5.1, and degree of the interpolating polynomial equals $m$;
- *for* $\alpha > 0$, we consider $\mathcal{N}_j^{\alpha,m}$ additional degrees of freedom (see (3.4)) that represent function evaluations for $j = 0$ and evaluations of the normal derivatives of order $j$ for $j > 0$ at distinct points in the interior of $\mathsf{e}$. This interior edge evaluations are in addition to the vertex ones already described. Tables 5.2 and 5.3 illustrates the cases for $\alpha = 1, 2$ and $\alpha + 1 < j \leq \alpha + 4$.

It turns out, that for the reconstructed polynomials $\partial_n^j v_{\mathsf{e}}(s)$ for $j = 0, 1, .., \alpha$ we can impose a total of $2(\alpha - j) + 2 + \mathcal{N}_j^{\alpha,m} = m - j + 1$ conditions. Therefore, as a general rule, for any pair $(\alpha, m)$ and a discrete field $v_{h|\mathsf{P}} \in \mathcal{V}_{\mathsf{P}}^{\alpha,m}$ we can uniquely determine on each edge $\mathsf{e} \in \partial\mathsf{P}$ the polynomials

$$\partial_n^j v_{\mathsf{e}}(s) \text{ of degree } m - j \ , \quad j = 0, 1, .., \alpha$$

that represent the reconstructed discrete function and its normal derivatives associated with $v_h$. We illustrate our reconstruction strategy with the following examples.

- For $\alpha = 1$, $m = 3$,

- $j = 0$, we consider the function values and the first derivatives at each vertex and we impose the *four* conditions

$$\begin{aligned} v_{\mathsf{e}}(0) &= v(\mathsf{v}'), & v_{\mathsf{e}}(|\mathsf{e}|) &= v(\mathsf{v}''), \\ v'_{\mathsf{e}}(0) &= \mathbf{t}_{\mathsf{e}} \cdot \nabla v(\mathsf{v}'), & v'_{\mathsf{e}}(|\mathsf{e}|) &= \mathbf{t}_{\mathsf{e}} \cdot \nabla v(\mathsf{v}''), \end{aligned}$$

  which allows us to build a *cubic* polynomial;

- $j = 1$, we consider the normal derivatives at each vertex and at the midpoint of the edge and we impose the *three* conditions:

$$\partial_n v(0) = \mathbf{t}_{\mathsf{e}} \cdot \nabla v(\mathsf{v}'), \quad \partial_n v(|\mathsf{e}|) = \mathbf{t}_{\mathsf{e}} \cdot \nabla v(\mathsf{v}''), \quad \text{and}$$

$$\partial_n v\left(|\mathsf{e}|/2\right) = \frac{\partial v(\mathbf{x}_{\mathsf{e}})}{\partial n},$$

  which allows us to build a *quadratic* polynomial.

- For $\alpha = 2$, $m = 4$,
  - $j = 0$, we consider the function values, the first and the second derivatives at each vertex and we impose the *six* conditions

$$\begin{aligned} v_{\mathsf{e}}(0) &= v(\mathsf{v}'), & v_{\mathsf{e}}(|\mathsf{e}|) &= v(\mathsf{v}''), \\ v'_{\mathsf{e}}(0) &= \mathbf{t}_{\mathsf{e}} \cdot \nabla v(\mathsf{v}'), & v'_{\mathsf{e}}(|\mathsf{e}|) &= \mathbf{t}_{\mathsf{e}} \cdot \nabla v(\mathsf{v}''), \\ v''_{\mathsf{e}}(0) &= \mathbf{t}_{\mathsf{e}} \cdot \nabla^2 v(\mathsf{v}')\mathbf{t}_{\mathsf{e}}, & v''_{\mathsf{e}}(|\mathsf{e}|) &= \mathbf{t}_{\mathsf{e}} \cdot \nabla^2 v(\mathsf{v}'')\mathbf{t}_{\mathsf{e}}, \end{aligned}$$

    which allows us to build a *fifth-order* polynomial;

  - $j = 1$, we consider the normal derivatives and their tangential derivatives at each vertex of the edge and we impose the *four* conditions:

$$\begin{aligned} \partial_n v(0) &= \mathbf{n}_{\mathsf{e}} \cdot \nabla v(\mathsf{v}'), & \partial_n v(|\mathsf{e}|) &= \mathbf{n}_{\mathsf{e}} \cdot \nabla v(\mathsf{v}''), \\ (\partial_n v)'(0) &= \mathbf{n}_{\mathsf{e}} \cdot \nabla^2 v(\mathsf{v}')\mathbf{t}_{\mathsf{e}}, & (\partial_n v)'(|\mathsf{e}|) &= \mathbf{n}_{\mathsf{e}} \cdot \nabla^2 v(\mathsf{v}'')\mathbf{t}_{\mathsf{e}}, \end{aligned}$$

    which allows us to build a *cubic* polynomial.

  - $j = 2$, we consider the second normal derivatives at each vertex and we impose the *two* conditions:

$$\partial_n^2 v(0) = \mathbf{n}_{\mathsf{e}} \cdot \nabla^2 v(\mathsf{v}')\mathbf{n}_{\mathsf{e}}, \qquad \partial_n^2 v(|\mathsf{e}|) = \mathbf{n}_{\mathsf{e}} \cdot \nabla^2 v(\mathsf{v}'')\mathbf{n}_{\mathsf{e}},$$

    which allows us to build a *linear* polynomial.

REMARK 5.3. *Let $v_h \in \mathcal{V}^h$. The trace reconstructions of $v_h$ and its normal derivatives on a edge $\mathsf{e}$ only depends on the degrees of freedom of $v_h$ associated with that edge, which are the same for $v_{h|\mathsf{P}_1}$ and $v_{h|\mathsf{P}_2}$ where $\mathsf{e} \subseteq \partial\mathsf{P}_1 \cap \partial\mathsf{P}_2$. In other words, the polynomials $\partial_n^j v_{\mathsf{e}}$, $j = 0, 1, .., \alpha$, built considering $\mathsf{e} \in \partial\mathsf{P}_1$ coincide with the corresponding polynomials built considering $\mathsf{e} \in \partial\mathsf{P}_2$.*

**5.3. Practical implementation of the stiffness matrix.** The construction of the stiffness matrix that corresponds to the bilinear form $\mathcal{A}_{h,\mathsf{P}}$ extends the algebraic construction of the low-order case presented in [17] to the higher order case in accordance with the more general framework of [34, Proposition 3.1]. A similar construction was originally proposed in [21] for the mixed formulation of the Poisson

problem and for other mimetic schemes in [9, 10, 5], see also [39]. Given $\mathsf{P} \in \Omega_h$, we build an elemental stiffness matrix $\mathsf{M}_\mathsf{P}$ such that

$$\mathcal{A}_{h,\mathsf{P}}\big(w_{h,\mathsf{P}}, v_{h,\mathsf{P}}\big) = w_{h,\mathsf{P}}^T\, \mathsf{M}_\mathsf{P}\, v_{h,\mathsf{P}} \qquad \forall w_{h,\mathsf{P}},\ v_{h,\mathsf{P}} \in \mathcal{V}_\mathsf{P}^{\alpha,m}.$$

The global stiffness matrix is obtained by a finite element-like assembly procedure.

To this purpose, we first construct two matrices $\mathsf{N}_\mathsf{P}$ and $\mathsf{R}_\mathsf{P}$ that satisfies an algebraic form of the consistency condition (S1), i.e., that are such that $\mathsf{M}_\mathsf{P}\mathsf{N}_\mathsf{P} = \mathsf{R}_\mathsf{P}$ and $\mathsf{N}_\mathsf{P}^T\mathsf{R}_\mathsf{P}$ is a symmetric and nonnegative definite matrix. Let $p_i$ be the $i$-th element of the basis $\mathcal{M}_m(\mathsf{P})$ for the polynomial space $\mathbb{P}_m(\mathsf{P})$. The index $i$ runs through 1 and $(m+1)(m+2)/2$ and suitably renumbers the monomials forming $\mathcal{M}_m(\mathsf{P})$, e.g.,

$$\begin{aligned} &p_1(x,y) = 1, \\ &p_2(x,y) = (x - x_\mathsf{P})/h_\mathsf{P}, \quad p_3(x,y) = (y - y_\mathsf{P})/h_\mathsf{P}, \quad \text{etc.} \end{aligned}$$

The center of the coordinate system has been conveniently set in the barycenter of the element $\mathsf{P}$. Let $(p_j)^\mathtt{I}$ be the interpolant of $p_j$ that returns the degrees of freedom in accordance with (4.1). Taking $\mathcal{N}_\mathsf{P}^{\alpha,m}$ degrees of freedom of $\mathcal{V}_\mathsf{P}^{\alpha,m}$ induced by (4.1), we define matrix $\mathsf{N}_\mathsf{P}$ in $\mathbb{R}^{m_{\mathcal{V}_\mathsf{P}^{\alpha,m}} \times n}$ by

$$\big(\mathsf{N}_\mathsf{P}\big)_{ij} = \text{ value of the } i^{th} \text{ degree of freedom of } (p_j)^\mathtt{I}.$$

On its turn, the columns of matrix $\mathsf{R}_\mathsf{P}$, which belongs to $\mathbb{R}^{m_{\mathcal{V}_\mathsf{P}^{\alpha,m}} \times n}$, represents the right-hand side of consistency condition (S1) applied to the polynomials $\big\{p_1, p_2, ...p_n\big\}$. Let $\varepsilon_{h,\mathsf{P}}^i$ indicate the unique vector in $\mathcal{V}_\mathsf{P}^{\alpha,m}$ whose $i$-th component is equal to one and the other ones are zero. Matrix $\mathsf{R}_\mathsf{P}$ takes the form:

$$\big(\mathsf{R}_\mathsf{P}\big)_{ij} = -\mathcal{I}_\mathsf{P}\big(\varepsilon_{h,\mathsf{P}}^j, p_j\big) + \sum_{\mathsf{e}\in\partial\mathsf{P}} \int_\mathsf{e} \varepsilon_{h,\mathsf{e}}^j(s) \pi_{m-1}^\mathsf{P}(\mathsf{K}\nabla p_j) \cdot \mathbf{n}_{\mathsf{P},\mathsf{e}}(s)\, dS$$

for $i = 1, \ldots, m_{\mathcal{V}_\mathsf{P}^{\alpha,m}}$ and $j = 1, \ldots, n$, and where as usual the functions $\varepsilon_{h,\mathsf{e}}^i(s)$ on the edges are the unique polynomials that interpolate the degrees of freedom as described in subsection 5.2.

Both matrices $\mathsf{N}_\mathsf{P}$ and $\mathsf{R}_\mathsf{P}$ are computable, and from the definitions above it is easy to prove that $\mathsf{M}_\mathsf{P}\mathsf{N}_\mathsf{P} = \mathsf{R}_\mathsf{P}$, which is the matrix form of the consistency condition (S2). Furthermore, a straightforward calculation shows that

$$\big(\mathsf{N}_\mathsf{P}^T\mathsf{R}_\mathsf{P}\big)_{ij} = \int_\mathsf{P} \mathsf{K}\nabla p_i \cdot \nabla p_j\, dV, \tag{5.12}$$

i.e. $\mathsf{N}_\mathsf{P}^T\mathsf{R}_\mathsf{P}$ is symmetric and semi-positive definite. Let $\mathsf{K}$ be the square symmetric matrix that represents the bilinear form $\mathcal{A}_h\big(\cdot,\cdot\big)$ restricted to the space $\mathbb{P}_m(\mathsf{P})$. Clearly, it holds that

$$\mathsf{K} = \mathsf{N}_\mathsf{P}^T\mathsf{M}_\mathsf{P}\mathsf{N}_\mathsf{P} = \mathsf{N}_\mathsf{P}^T\mathsf{R}_\mathsf{P}, \tag{5.13}$$

where matrix $\mathsf{K}$ has the block-diagonal form

$$\mathsf{K} = \begin{pmatrix} 0 & \mathbf{0} \\ \mathbf{0} & \widehat{\mathsf{K}} \end{pmatrix}$$

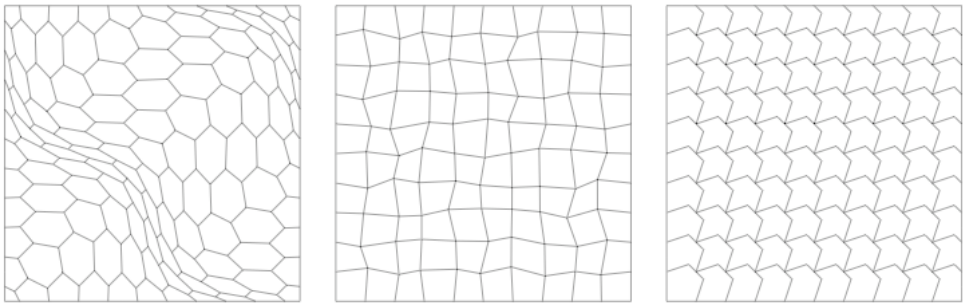

FIG. 6.1. *Poisson problem on the square domain* $[0,1]\times[0,1]$*; from left to right: the mainly-hexagonal mesh* ($\mathcal{M}_2$)*, the mesh of randomized quadrilaterals* ($\mathcal{M}_1$)*, and the non-convex mesh corresponding to second refinement level* ($\mathcal{M}_3$)*.*

| $l$ | $N_{\mathsf{P}}$ | $N_{\mathsf{e}}$ | $N_{\mathsf{v}}$ | #dofs | $h$ |
|---|---|---|---|---|---|
| 1 | 36 | 125 | 90 | 251 | $3.405\,10^{-1}$ |
| 2 | 121 | 400 | 280 | 801 | $2.008\,10^{-1}$ |
| 3 | 441 | 1400 | 960 | 2801 | $1.071\,10^{-1}$ |
| 4 | 1681 | 5200 | 3520 | 10401 | $5.422\,10^{-2}$ |
| 5 | 6561 | 20000 | 13440 | 40001 | $2.719\,10^{-2}$ |
| 6 | 25921 | 78400 | 52480 | 156801 | $1.361\,10^{-2}$ |

TABLE 6.1

*Mesh data for the sequence* $\mathcal{M}_1$ *of meshes with mainly hexagonal cells;* $l$ *is the refinement level,* $N_{\mathsf{P}}$ *is the number of cells,* $N_{\mathsf{e}}$ *is the number of edges,* $N_{\mathsf{v}}$ *is the number of vertices,* #dofs *is the number of degrees of freedom,* $h$ *is the mesh size.*

and $\widehat{\mathsf{K}}\in\mathbb{R}^{(n-1)\times(n-1)}$ is a strictly positive definite matrix. More precisely, matrix $\widehat{\mathsf{K}}$ is the strictly positive definite matrix that is given by (5.12) if we exclude $i=1$ and $j=1$, i.e., the constant polynomial $p_1(x,y)=1$. Let $\mathsf{K}^\dagger\in\mathbb{R}^{n\times n}$ be the pseudo-inverse of matrix $\mathsf{K}$, which we define as

$$\mathsf{K}^\dagger=\begin{pmatrix}0 & \mathbf{0}\\ \mathbf{0} & \widehat{\mathsf{K}}^{-1}\end{pmatrix}.$$

Eventually, we define the local stiffness matrix

$$\mathsf{M}_{\mathsf{P}}=\mathsf{R}_{\mathsf{P}}\mathsf{K}^\dagger\mathsf{R}_{\mathsf{P}}^T+\alpha\mathsf{P}_{\mathsf{P}}, \tag{5.14}$$

where the positive scalar $\alpha$ is equal to the trace of $\mathsf{R}_{\mathsf{P}}\mathsf{K}^\dagger\mathsf{R}_{\mathsf{P}}^T$, and

$$\mathsf{P}_{\mathsf{P}}=\mathsf{I}-\mathsf{N}_{\mathsf{P}}\big(\mathsf{N}_{\mathsf{P}}^T\mathsf{N}_{\mathsf{P}}\big)^{-1}\mathsf{N}_{\mathsf{P}}^T,$$

where $\mathsf{I}$ is the (properly sized) identity matrix. Note that matrix $\mathsf{P}_{\mathsf{P}}$ is the projector on the space orthogonal to the space spanned by the columns of matrix $\mathsf{N}_{\mathsf{P}}$ and that the product $\mathsf{P}_{\mathsf{P}}\mathsf{N}_{\mathsf{P}}$ is zero.

**6. Numerical Experiments.** The numerical experiments presented in this section are designed to confirm the *a priori* analysis developed in the previous section in a general setting. In particular, when we use a method corresponding to the pair $(\alpha,m)$ the numerical solution is expected to behave like an $m$-order accurate approximation

| $l$ | $N_{\mathsf{P}}$ | $N_{\mathsf{e}}$ | $N_{\mathsf{v}}$ | #dofs | $h$ |
|---|---|---|---|---|---|
| 1 | 25 | 60 | 36 | 121 | $3.311\,10^{-1}$ |
| 2 | 100 | 220 | 121 | 441 | $1.865\,10^{-1}$ |
| 3 | 400 | 840 | 441 | 1681 | $9.412\,10^{-2}$ |
| 4 | 1600 | 3280 | 1681 | 6561 | $4.693\,10^{-2}$ |
| 5 | 6400 | 12960 | 6561 | 25921 | $2.389\,10^{-2}$ |
| 6 | 25600 | 51520 | 25921 | 103041 | $1.221\,10^{-2}$ |

TABLE 6.2

*Mesh data for the sequence $\mathcal{M}_2$ of randomized quadrilateral meshes; $l$ is the refinement level, $N_{\mathsf{P}}$ is the number of cells, $N_{\mathsf{e}}$ is the number of edges, $N_{\mathsf{v}}$ is the number of vertices, #dofs is the number of degrees of freedom, $h$ is the mesh size.*

| $l$ | $N_{\mathsf{P}}$ | $N_{\mathsf{e}}$ | $N_{\mathsf{v}}$ | #dofs | $h$ |
|---|---|---|---|---|---|
| 1 | 25 | 120 | 96 | 241 | $2.915\,10^{-1}$ |
| 2 | 100 | 440 | 341 | 881 | $1.458\,10^{-1}$ |
| 3 | 400 | 1680 | 1281 | 3361 | $7.289\,10^{-2}$ |
| 4 | 1600 | 6560 | 4961 | 13121 | $3.644\,10^{-2}$ |
| 5 | 6400 | 25920 | 19521 | 51841 | $1.822\,10^{-2}$ |
| 6 | 25600 | 103040 | 77441 | 206081 | $9.111\,10^{-3}$ |

TABLE 6.3

*Mesh data for the sequence $\mathcal{M}_3$ of meshes with non-convex cells; $l$ is the refinement level, $N_{\mathsf{P}}$ is the number of cells, $N_{\mathsf{e}}$ is the number of edges, $N_{\mathsf{v}}$ is the number of vertices, #dofs is the number of degrees of freedom, $h$ is the mesh size.*

of the exact solution, assuming that this latter one is at least $H^{1+\alpha}$-regular. Therefore, the convergence rate is expected to be of order $\mathcal{O}(h^m)$ if the error is measured in the following mesh-dependent norm

$$\|v_h\|_{1,h}^2 = \sum_{\mathsf{P}\in\Omega_h} \|v_h\|_{1,h,\mathsf{P}}^2, \tag{6.1}$$

where each term $\|v_h\|_{1,h,\mathsf{P}}^2$ is a local approximation of the square of the energy seminorm of $v_h$. For $m \geq 2$, this local contribution reads as:

$$\begin{aligned}\|v_h\|_{1,h,\mathsf{P}}^2 = &\sum_{\mathsf{e}\in\partial\mathsf{P}} h_{\mathsf{P}}\,|v_h|_{H^1(\mathsf{e})}^2 + \sum_{j=1}^{\alpha}\sum_{\mathsf{e}\in\partial\mathsf{P}} h_{\mathsf{P}}^{2j-1}\|\partial_n^j v_{\mathsf{e}}\|_{L^2(\mathsf{e})}^2 \\ &+ \Big(\frac{1}{|\mathsf{P}|}\int_{\mathsf{P}} v_h\,dV - \overline{v}_{h,\mathsf{P}}\Big)^2 + \sum_{j=1}^{m-2}\sum_{q\in\mathcal{M}_j(\mathsf{P})}\Big(\frac{1}{|\mathsf{P}|}\int_{\mathsf{P}} v_h q\,dV\Big)^2,\end{aligned} \tag{6.2}$$

where $\overline{v}_{h,\mathsf{P}}$ is the arithmetic mean of the values that $v_h$ takes at the $N_{\mathsf{P}}^{\mathcal{V}}$ vertices of the element $\mathsf{P}$ (here denoted by $v_{\mathsf{v}}$), i.e.,

$$\overline{v}_{h,\mathsf{P}} = \frac{1}{N_{\mathsf{P}}^{\mathcal{V}}}\sum_{\mathsf{v}\in\partial\mathsf{P}} v_{\mathsf{v}}. \tag{6.3}$$

For $m = 1$, the last two summation terms in (6.2) must be neglected. Recalling Theorem 4.1 and Corollary 4.2 it is easy to check that, under the same hypotheses, the rate of convergence in the (6.1) norm will satisfy

$$\|u_h - u\|_{1,h,\mathsf{P}}^2 \leq Ch^m\,|u|_{m+1}\,,$$

as it holds for the $H^1$-norm. Moreover, we expect this error bound to be sharp.

We solve the diffusion problem (2.1)-(2.2) on the domain $\Omega = ]0,1[\times]0,1[$ and Dirichlet conditions assigned on all the domain boundary $\Gamma$. The right-hand side $f$ and the boundary function $g$ are determined in accordance with the exact solution

$$u(x,y) = x\sin(2\pi x)\sin(2\pi y) + x^3y^2, \tag{6.4}$$

and the diffusion tensor:

$$\mathsf{K}(x,y) = \begin{pmatrix} +1+y^2 & -xy \\ -xy & 1+x^2 \end{pmatrix}. \tag{6.5}$$

The performance of the nodal MFD method is investigated by evaluating the rate of convergence on four families of two-dimensional refined meshes. The second mesh in each family is shown in Fig. 6.1 and the data of the refined meshes are given in Tables 6.1, 6.2 and 6.3. In these tables, the columns labeled by $N_{\mathsf{P}}$, $N_{\mathsf{e}}$ and $N_{\mathsf{v}}$ report the numbers of mesh cells, edges and vertices, respectively, $\#\mathsf{dofs}$ is the number of degrees of freedom and $h$ is the mesh size parameter.

Let us briefly describe the construction of these mesh families. The meshes in $\mathcal{M}_1$ are built by dualization of a regular triangular mesh after a smooth coordinate transformation. This kind of meshes is rather common in the mimetic literature, see for example [10]. To this purpose, we remap the position $(\widehat{x},\widehat{y})$ of the nodes of a uniform partition by the smooth coordinate transformation:

$$\begin{aligned} x &= \widehat{x} + (1/10)\sin(2\pi\widehat{x})\sin(2\pi\widehat{y}), \\ y &= \widehat{y} + (1/10)\sin(2\pi\widehat{x})\sin(2\pi\widehat{y}). \end{aligned} \tag{6.6}$$

The meshes in $\mathcal{M}_1$ are built from the "primal" mesh at level $l$ by splitting each quadrilateral cell into two triangles and connecting the barycenters of adjacent triangular cells by a straight segment. The mesh construction is completed at the boundary $\Gamma$ by connecting the barycenters of the triangular cells close to $\Gamma$ to the midpoints of the boundary edges and these latters to the boundary vertices of the "primal" mesh. The left-most plot of Figure 6.1 shows the second refinement mesh of $\mathcal{M}_1$, which is built from an initial $10\times 10$ regular partition.

The meshes in $\mathcal{M}_2$ are built by randomly perturbing an underlying uniform partition of the domain $\Omega$ formed by square-shaped elements. Since the randomization is carried out independently at every mesh refinement, there is no mesh regularization effect in the process as occurs for example when a quadrilateral is split into four subcells by joining the midpoints of opposited edges. The middle plot of Figure 6.1 shows the second refinement mesh of $\mathcal{M}_2$, which is built from an initial $10\times 10$ regular partition.

As shown in the right-most plot of Figure 6.1, a non-convex mesh of $\mathcal{M}_3$ is made of a regular pattern of octagonal cells, which are built by adding a mesh vertex at each edge midpoint of an underlying square mesh. This additional vertex is then translated by a fixed displacement vector when the original position lies inside the computational domain. The right-most plot of Figure 6.1 shows the second refinement mesh of $\mathcal{M}_3$, which is built from an initial $10\times 10$ regular partition. The simulation data of the meshes used in these numerical calculation are summarized in Tables 6.1, 6.2 and 6.3.

The numerical results are shown in Figures 6.2, 6.3, and 6.4 for, respectively, mesh families $\mathcal{M}_1$, $\mathcal{M}_2$, and $\mathcal{M}_3$. In each figures, we show the error curves for the

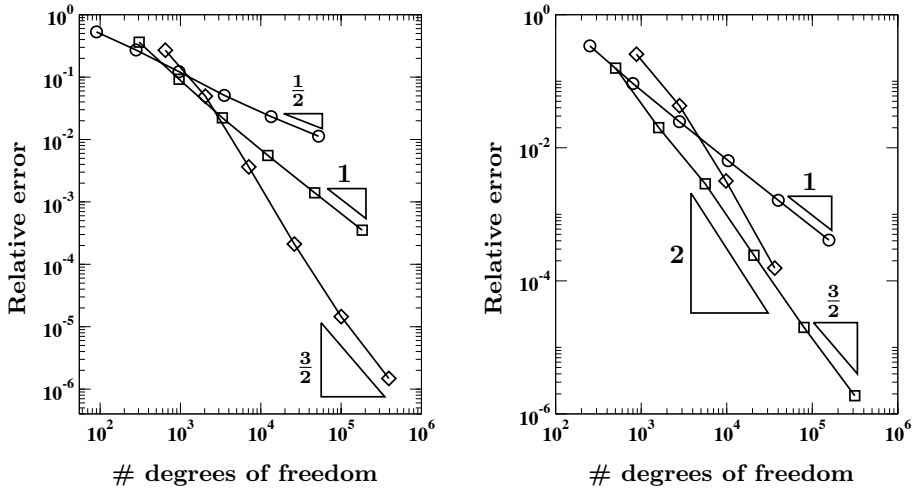


FIG. 6.2. *Poisson problem on the square domain* $[0,1]\times[0,1]$ *with variable permeability using the mesh family* $\mathcal{M}_1$ *(mainly hexagonal meshes); the error curves corresponds to the schemes labeled by* $(\alpha, m)$ *with* $\alpha = 0$ *(circles),* $\alpha = 1$ *(squares),* $\alpha = 2$ *(diamonds) and* $m = \alpha + 1$ *(left plot),* $m = \alpha + 2$ *(right plot); expected rates are of order* $\mathcal{O}(N^{-\nu})$ *with* $\nu = m/2$ *(since* $N \approx h^{-2}$*); exact slopes corresponding to* $\nu$ *are shown in each plot for comparison.*

numerical approximation that are obtained by the applying virtual element schemes corresponding to the pair of indices $(\alpha, m)$ with $\alpha = 0, 1, 2$ and $m = \alpha + 1$ (left plots) and $m = \alpha + 2$ (right plots), see the captions for more details. The relative errors, which are measured by using the norm defined in (6.1), are plotted against $N$, the total number of degrees of freedom. The convergence rate on each mesh sequence is reflected by the slope of the corresponding error curve, and is expected to be of order $\mathcal{O}(N^{m/2})$ asymptotically, since $N \approx h^2$. In each we show, for comparison, the theoretical slope and we also indicate the exponent. All these plots essentially confirm the good behavior of the schemes that we propose in this paper.

**7. Conclusions.** In this work, we proposed and analyzed a virtual element method that is suitable to the numerical approximation of second-order diffusion problems with variable coefficients and provides arbitrary regular discrete solutions. The numerical approximation can be of arbitrary order, the optimality being dependent on the regularity of the exact solution. Numerical results confirm the effectiveness of the approach.

As pointed out in the introduction and remarked throughout the paper, the possibility to build such methods quite easily is one of the major properties of the virtual element method and, with respect to this issue, this work is to be intended as a first contribution to the virtual finite element literature. We emphasize that the virtual element method opens a wide range of exciting applications, as, for example, easier discretizations of higher order problems, direct calculation of derived quantities such as fluxes, strains, stresses, etc., that may exactly correspond to some of the degrees of freedom of the numerical solution, anisotropic error estimation based on the Hessian of the solution, better eigenvalue approximation, numerical treatment of the stream

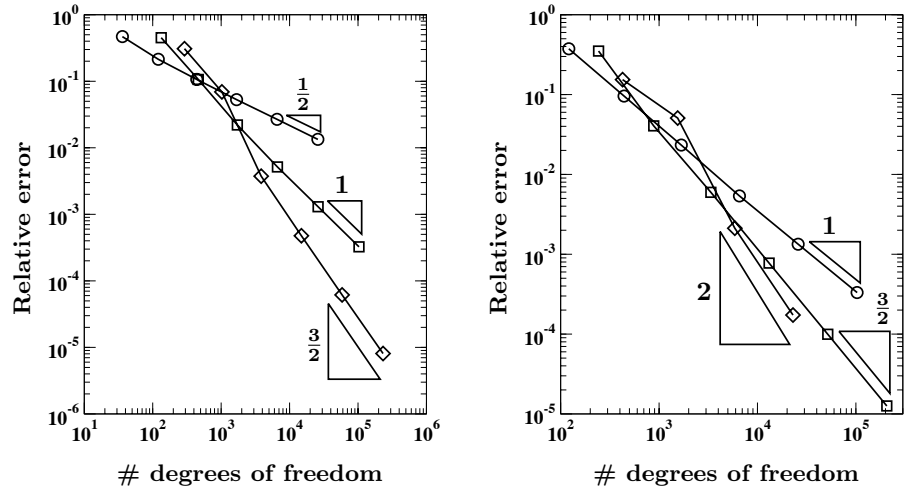


FIG. 6.3. *Poisson problem on the square domain* $[0,1]\times[0,1]$ *with variable permeability using the mesh family* $\mathcal{M}_2$ *(randomized quadrilateral meshes); the error curves corresponds to the schemes labeled by* $(\alpha, m)$ *with* $\alpha = 0$ *(circles),* $\alpha = 1$ *(squares),* $\alpha = 2$ *(diamonds) and* $m = \alpha + 1$ *(left plot),* $m = \alpha + 2$ *(right plot); expected rates are of order* $\mathcal{O}(N^{-\nu})$ *with* $\nu = m/2$ *(since* $N \approx h^{-2}$*); exact slopes corresponding to* $\nu$ *are shown in each plot for comparison.*

function formulation of the Stokes problem, where velocities are described as curls of $C^1$ scalar fields, etc. Finally, the present construction makes it possible a general "*hkp* approach", i.e. a method in which the polynomial degree may vary from element to element and the regularity index $\alpha$ may vary from edge to edge.

## Acknowledgements

The work of the second author was partially supported by the National Nuclear Security Administration of the U.S. Department of Energy at Los Alamos National Laboratory under Contract No. DE-AC52-06NA25396 and the DOE Office of Science Advanced Scientific Computing Research (ASCR) Program in Applied Mathematics.

REFERENCES

[1] P.F. Antonietti, L. Beirão da Veiga, and M. Verani. A mimetic discretization of elliptic obstacle problems, 2012. to appear.

[2] J. H. Argyris, I. Fried, and D. W. Scharpf. The TUBA family of plate elements for the matrix displacement method. *Areonaut. J. ROY. Areonaut. Soc.*, 72:701–709, 1968.

[3] E. D. Batista and J. E. Castillo. Mimetic schemes on non-uniform structured meshes. *Electronic Transactions on Numerical Analysis*, 34:152–162, 2009.

[4] L. Beirão da Veiga. A residual based error estimator for the mimetic finite difference method. *Numer. Math.*, 108(3):387–406, 2008.

[5] L. Beirão da Veiga. A mimetic discretization method for linear elasticity. *Math. Mod. and Numer. Anal.*, 44(2):231–250, 2010.

[6] L. Beirão da Veiga, F. Brezzi, A. Cangiani, G. Manzini, L. D. Marini, and A. Russo. The Virtual Element Method. *Math. Models Methods Appl. Sci.*, 2013. (to appear).

[7] L. Beirão da Veiga, F. Brezzi, and L. D. Marini. Virtual Elements for linear elasticity problems. Technical Report Preprint IMATI 11cPV12/10/0, IMATI-CNR, 2011.

[8] L. Beirão da Veiga, J. Droniou, and G. Manzini. A unified approach to handle convection term

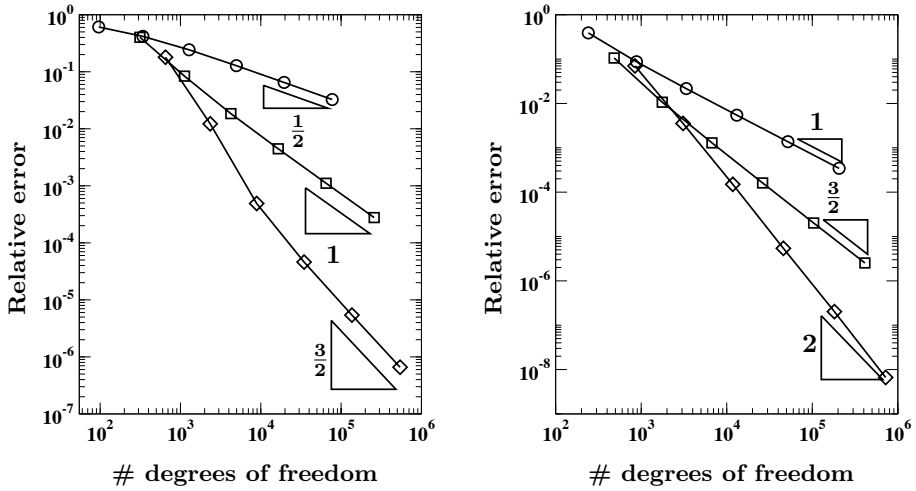


FIG. 6.4. *Poisson problem on the square domain* $[0,1]\times[0,1]$ *with variable permeability using the mesh family* $\mathcal{M}_3$ *(non-convex polygon meshes); the error curves corresponds to the schemes labeled by* $(\alpha, m)$ *with* $\alpha = 0$ *(circles),* $\alpha = 1$ *(squares),* $\alpha = 2$ *(diamonds) and* $m = \alpha + 1$ *(left plot),* $m = \alpha + 2$ *(right plot); expected rates are of order* $\mathcal{O}(N^{-\nu})$ *with* $\nu = m/2$ *(since* $N \approx h^{-2}$*); exact slopes corresponding to* $\nu$ *are shown in each plot for comparison.*

in finite volumes and mimetic discretization methods for elliptic problems. *IMA J. Num. Anal.*, 31(4):1357–1401, 2011.

[9] L. Beirão da Veiga, V. Gyrya, K. Lipnikov, and G. Manzini. Mimetic finite difference method for the Stokes problem on polygonal meshes. *J. Comput. Phys.*, 228(19):7215–7232, 2009.

[10] L. Beirão da Veiga, K. Lipnikov, and G. Manzini. Convergence analysis of the high-order mimetic finite difference method. *Numer. Math.*, 113(3):325–356, 2009.

[11] L. Beirão da Veiga, K. Lipnikov, and G. Manzini. Error analysis for a Mimetic Discretization of the steady Stokes problem on polyhedral meshes. *SIAM J. Numer. Anal.*, 48:1419–1443, 2011.

[12] L. Beirão da Veiga, K. Lipnikov, and G. Manzini. High-order nodal mimetic discretizations of elliptic problems on polygonal meshes. *SIAM Journal on Numerical Analysis*, 49(5):1737–1760, 2011.

[13] L. Beirão da Veiga and G. Manzini. An a posteriori error estimator for the mimetic finite difference approximation of elliptic problems. *Int. J. Numer. Meth. Engrg.*, 76(11):1696–1723, 2008.

[14] L. Beirão da Veiga and G. Manzini. A higher-order formulation of the mimetic finite difference method. *SIAM Journal on Scientific Computing*, 31(1):732–760, 2008.

[15] K. Bell. A refined triangular plate bending finite element. *Internat. J. Numer. Meth. Engrg.*, 1:101–122, 1969.

[16] S. C. Brenner and L. R. Scott. *The mathematical theory of finite element methods*, volume 15 of *Texts in Applied Mathematics*. Springer, New York, third edition, 2008.

[17] F. Brezzi, A. Buffa, and K. Lipnikov. Mimetic finite differences for elliptic problems. *M2AN Math. Model. Numer. Anal.*, 43(2):277–295, 2009.

[18] F. Brezzi, A. Buffa, and G. Manzini. Mimetic scalar products for discrete differential forms, 2012.

[19] F. Brezzi and Marini. L.D. Virtual element method for plate bending problems, 2012. Submitted.

[20] F. Brezzi, K. Lipnikov, and M. Shashkov. Convergence of the mimetic finite difference method for diffusion problems on polyhedral meshes. *SIAM J. Numer. Anal.*, 43(5):1872–1896, 2005.

[21] F. Brezzi, K. Lipnikov, and V. Simoncini. A family of mimetic finite difference methods on

polygonal and polyhedral meshes. *Math. Models Methods Appl. Sci.*, 15(10):1533–1551, 2005.

[22] A. Cangiani, F. Gardini, and G. Manzini. Convergence of the mimetic finite difference method for eigenvalue problems in mixed form. *Comput. Methods Appl. Mech. Engrg.*, 200((9-12)):1150–1160, 2010.

[23] A. Cangiani and G. Manzini. Flux reconstruction and pressure post-processing in mimetic finite difference methods. *Comput. Methods Appl. Mech. Engrg.*, 197/9-12:933–945, 2008.

[24] A. Cangiani, G. Manzini, and A. Russo. Convergence analysis of the mimetic finite difference method for elliptic problems. *SIAM J. Numer. Anal.*, 47(4):2612–2637, 2009.

[25] J. Castillo, J. Hyman, M. Shashkov, and S. Steinberg. The sensitivity and accuracy of fourth order finite-difference schemes on nonuniform grids in one dimension. *An International Journal of Computers & Mathematics with Applications*, 30(8):41–55, 1995.

[26] J. Castillo, J. Hyman, M. Shashkov, and S. Steinberg. Fourth- and sixth-order conservative finite-difference approximations of the divergence and gradient. *Applied Numerical Mathematics*, 37:171–187, 2001.

[27] J. E. Castillo and R. D. Grone. A matrix analysis approach to higher-order approximations for divergence and gradients satisfying a global conservation law. *SIAM. J. Matrix Anal. Appl.*, 25(1):128–142, 2003.

[28] J.E. Castillo, J.M. Hyman, M.J. Shashkov, and S. Steinberg. High-order mimetic finite difference methods on nonuniform grids. *Special Issue of Houston Journal of Mathematics*, eds. A.V. Ilin and L. R. Scott:347–361, 1995.

[29] P.G. Ciarlet. *The finite element method for elliptic problems.* North-Holland, Amsterdam, 1978.

[30] R..W. Clough and J. L. Tocher. Finite element stiffness matrices for analysis of plates in bending. In *Proceedings of the Conference of Matrix Methods in Structural Mechanics*, Wright Patterson A.F.B. Ohio, 1965.

[31] J. A. Cottrell, T. J. R. Hughes, and Y. Bazilevs. *Isogeometric Analysis. Towards integration of CAD and FEA.* Wiley, 2009.

[32] C. de Boor. *A practical guide to splines.* Springer, 2001.

[33] P. Grisvard. *Elliptic problems in nonsmooth domains*, volume 24 of *Monographs and Studies in Mathematics.* Pitman, Boston, 1985.

[34] K. Lipnikov, G. Manzini, F. Brezzi, and A. Buffa. The mimetic finite difference method for 3D magnetostatics fields problems. *J. Comput. Phys.*, 230(2):305–328, 2011.

[35] K. Lipnikov, G. Manzini, and D. Svyatskiy. Analysis of the monotonicity conditions in the mimetic finite difference method for elliptic problems. *J. Comput. Phys.*, 230(7):2620 – 2642, 2011.

[36] L. L. Schumaker. *Spline Functions: Basic Theory.* Cambridge University Press, third edition edition, 2007.

[37] M. Shashkov and S. Steinberg. Support-operator finite-difference algorithms for general elliptic problems. *J. Comput. Phys.*, 118(1):131 – 151, 1995.

[38] M. Shashkov and S. Steinberg. Solving diffusion equations with rough coefficients in rough grids. *Journal of Computational Physics*, 129(2):383 – 405, 1996.

[39] K.A. Trapp. Inner products in covolume and mimetic methods. *M2AN: Math. Model. Numer. Anal.*, 42:941–959, 2008.